ISSN: 2161-6795 Volume 10, Number 1, January 2020

Scientific Research Publishing

World Journal of Nuclear Science and Technology

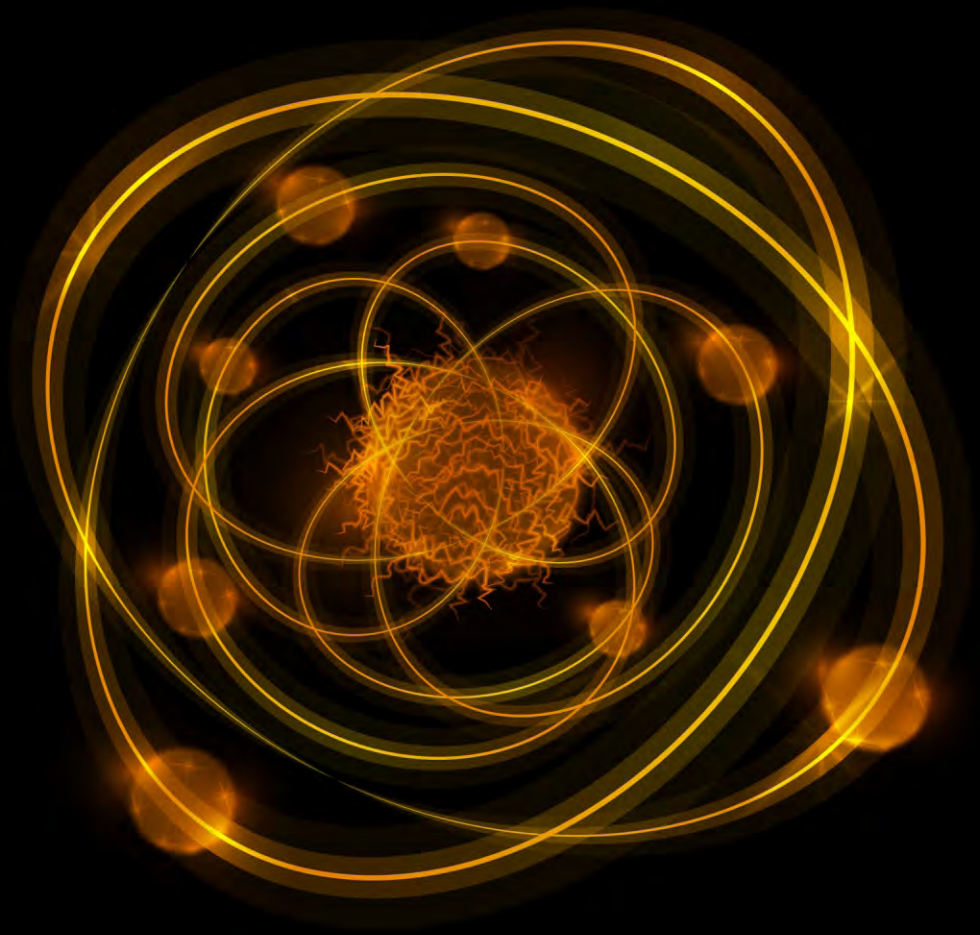

ISSN: 2161-6795

https://www.scirp.org/journal/wjnst

Journal Editorial Board

ISSN 2161-6795 (Print) ISSN 2161-6809 (Online)
https://www.scirp.org/journal/wjnst

Editor-in-Chief

Prof. Andrzej Grzegorz Chmielewski — Institute of Nuclear Chemistry and Technology, Poland

Editorial Board

Dr. Abdullah Aydin — Kirikkale University, Turkey
Prof. Jiejin Cai — Sun Yat-sen University, China
Prof. Ahmet Cengiz — Uluda University, Turkey
Prof. Abdelmajid Choukri — University of Ibn Tofail, Morocco
Prof. Snezana Dragovic — University of Belgrade, Serbia
Prof. Hardy Christian Ekberg — Chalmers University of Technology, Sweden
Prof. Juan-Luis François — National Autonomous University of Mexico, Mexico
Prof. Shilun Guo — China Institute of Atomic Energy, China
Prof. Shaban Ramadan Mohamed Harb — South Valley University, Egypt
Prof. Xiaolin Hou — Technical University of Denmark, Denmark
Prof. Ning Liu — Sichuan University, China
Prof. Man Gyun Na — Chosun University, South Korea
Prof. Dragoslav Nikezic — University of Kragujevac, Serbia
Dr. Rafael Rodríguez Pérez — University of Las Palmas de Gran Canaria, Spain
Prof. K. Indira Priyadarsini — Bhabha Atomic Research Centre, India
Prof. Massimo Rogante — Studio d'Ingegneria Rogante, Italy
Prof. Vitalii D. Rusov — Odessa National Polytechnic University, Ukraine
Dr. Chhanda Samanta — Virginia Military Institute, USA
Prof. Kune Y. Suh — Seoul National University, South Korea
Prof. Wenxi Tian — Xi'an Jiaotong University, China
Dr. Heiko Timmers — The University of New South Wales, Australia
Prof. Marco Túllio Menna Barreto de Vilhena — Federal University of Rio Grande do Sul, Brazil
Dr. Jun Wang — University of Wisconsin Madison, USA
Dr. Leopoldo A. Pando Zayas — University of Michigan, USA

Scientific Research Publishing

World Journal of Nuclear Science and Technology, 2020, 10, 1-64
https://www.scirp.org/journal/wjnst
ISSN Online: 2161-6809
ISSN Print: 2161-6795

Table of Contents

Volume 10 Number 1 January 2020

World Journal of Nuclear Science and Technology (WJNST)
Journal Information

SUBSCRIPTIONS

The *World Journal of Nuclear Science and Technology* (Online at Scientific Research Publishing, https://www.scirp.org/) is published quarterly by Scientific Research Publishing, Inc., USA.

Subscription rates:
Print: $79 per issue.
To subscribe, please contact Journals Subscriptions Department, E-mail: sub@scirp.org

SERVICES

Advertisements
Advertisement Sales Department, E-mail: service@scirp.org

Reprints (minimum quantity 100 copies)
Reprints Co-ordinator, Scientific Research Publishing, Inc., USA.
E-mail: sub@scirp.org

COPYRIGHT

Copyright and reuse rights for the front matter of the journal:
Copyright © 2020 by Scientific Research Publishing Inc.
This work is licensed under the Creative Commons Attribution International License (CC BY).
http://creativecommons.org/licenses/by/4.0/

Copyright for individual papers of the journal:
Copyright © 2020 by author(s) and Scientific Research Publishing Inc.

Reuse rights for individual papers:
Note: At SCIRP authors can choose between CC BY and CC BY-NC. Please consult each paper for its reuse rights.

Disclaimer of liability
Statements and opinions expressed in the articles and communications are those of the individual contributors and not the statements and opinion of Scientific Research Publishing, Inc. We assume no responsibility or liability for any damage or injury to persons or property arising out of the use of any materials, instructions, methods or ideas contained herein. We expressly disclaim any implied warranties of merchantability or fitness for a particular purpose. If expert assistance is required, the services of a competent professional person should be sought.

PRODUCTION INFORMATION

For manuscripts that have been accepted for publication, please contact:
E-mail: wjnst@scirp.org

World Journal of Nuclear Science and Technology, 2020, 10, 1-8
https://www.scirp.org/journal/wjnst
ISSN Online: 2161-6809
ISSN Print: 2161-6795

Elastic Cross Sections for ^{3}He + ^{58}Ni above the Coulomb Barrier

R. Arceo[1], Omar Pedraza[2], Luis M. Sandoval[1], L. A. López[2], C. Álvarez[1], F. Hueyotl-Zahuantitla[1,3], Ariel Flores-Rosas[1], G. Luis Raya[4], Jesús Martínez-Castro[5]

[1]Facultad de Ciencias en Física y Matemáticas, Universidad Autónoma de Chiapas, Tuxtla Gutiérrez, México
[2]Area Académica de Matemáticas y Física, Universidad Autónoma del Estado de Hidalgo, Pachuca, México
[3]CONACYT, México City, México
[4]Universidad Politécnica de Pachuca, Pachuca, México
[5]Centro de Investigación en Computación, Instituto Politécnico Nacional, México City, México
Email: roberto.arceo@unach.mx, lsandovalm@yahoo.com, crabpulsar@hotmail.com, aros8151@gmail.com, omarp@uaeh.edu.mx, lalopez@uaeh.edu.mx, gilgamesh@upp.edu.mx, macj@cic.ipn.mx, filihz@gmail.com

How to cite this paper: Arceo, R., Pedraza, O., Sandoval, L.M., López, L.A., Álvarez, C., Hueyotl-Zahuantitla, F., Flores-Rosas, A., Raya, G.L. and Martínez-Castro, J. (2020) Elastic Cross Sections for ^{3}He + ^{58}Ni above the Coulomb Barrier. *World Journal of Nuclear Science and Technology*, **10**, 1-8.
https://doi.org/10.4236/wjnst.2020.101001

Received: September 25, 2019
Accepted: November 8, 2019
Published: November 11, 2019

Copyright © 2020 by author(s) and Scientific Research Publishing Inc.
This work is licensed under the Creative Commons Attribution International License (CC BY 4.0).
http://creativecommons.org/licenses/by/4.0/
Open Access

Abstract

In this work, the elastic cross section is calculated at energies above the Coulomb barrier for ^{3}He + ^{58}Ni using a Woods-Saxon potential. The solutions of the radial Schrödinger equations are calculated numerically and they are introduced in the S matrix, after which the cross section is obtained. The parameters in the potential are adjusted to satisfy known experimental data.

Keywords

Elastic and Inelastic Scattering, Scattering Theory, Total Cross Sections

1. Introduction

We have studied the scattering of nuclei by helium and nickel atoms using the Schrödinger equation at energies up to 35 MeV for the reaction ^{3}He + ^{58}Ni using a radial Woods-Saxon potential. We treated the Schrödinger equation numerically, for the case of the *Woods-Saxon* potential [1]; the parameters for this potential were adjusted to coincide with known experimental data.

The value of chi-squared was minimized by using a theoretical model and the experimental data from Fujisawa *et al.* [2]. The parameters thus obtained are used in the Woods-Saxon potential and we compare the results with known experimental data.

Recently we have results at low energies for the reaction ^{3,4,6}He + ^{58}Ni [2] [3] [4] [5]. We compare our results for this reaction and show that the Woods-Saxon

potential agrees with known experimental data.

This paper is divided into four sections as follows. In Section 2, we briefly describe the setup; Section 2.1 is dedicated to obtaining the Woods-Saxon potential. In Section 2.2, we discuss the elastic cross section for the scattering of helium by nickel atoms. In Section 3, the obtained results are shown. Finally, in Section 4 we focus on the discussion of our results.

2. Theory

In this section we describe the procedure used to compute the Woods-Saxon potential produced by a point particle. We then calculate the cross section for the collision of two particles of mass $m_{1,2}$ and atomic number $Z_{1,2}$. Our approach to this problem is numerical, and we make the assumption that the interaction of the incident particle with the rest atom can be accounted for by the effective Woods-Saxon potential which we calculate below. We minimize the value of chi squared from the experimental ^{3}He + ^{58}Ni data [2] and the parameters we obtain are shown in Table 1 and Table 2.

2.1. The Woods-Saxon Potential

The Woods-Saxon potential is a mean field potential for the nucleons (protons and neutrons) inside the atomic nucleus, which is used to describe approximately the forces applied on each nucleon, in the nuclear shell model for the structure of the nucleus.

The standard Woods-Saxon potential [1], as a function of the distance r^* from the nuclear center, is defined by:

$$V'\left(r^*\right) = -\frac{V_0}{1+\exp\left(\frac{r^*-R}{a}\right)}, a \ll R \tag{1}$$

Table 1. Parameters obtained for the reaction ^{3}He + ^{58}Ni.

E	l	V_0	R_1	a_1	W_0	R_2	a_2	σ_R	σ_T	χ^2/N
(MeV)	up to	(MeV)	(fm)	(fm)	(MeV)	(fm)	(fm)	(mb)	(mb)	
24.15	11	174.400	1.30	0.750	17.1	1.41	0.71	1476.904	2871.663	11.95
27.64	15	174.275	0.93	0.601	17.1	1.41	0.71	1526.071	3542.422	5.85
34.14	13	174.500	0.94	0.75	18.6	1.41	0.73	1620.872	2695.711	2.21

Table 2. Parameters obtained with the derivative in the complex term of the Woods-Saxon potential for the reaction ^{3}He + ^{58}Ni.

E	l	V_0	R_1	a_1	W_0	R_2	a_2	σ_T	χ^2/N
(MeV)	up to	(MeV)	(fm)	(fm)	(MeV)	(fm)	(fm)	(mb)	
24.15	11	175.0	1.3	0.75	18.2	1.41	0.72	3277.768	17.903
27.64	15	173.6	1.3	0.75	17.1	1.41	0.71	3046.658	5.047
34.14	13	173.9	0.94	0.75	18.9	1.41	0.73	2804.289	1.832

where V_0 (with dimensions of energy, MeV) represents the potential well depth, *a* is a length representing the "surface thickness" of the nucleus, and $R = r_0 A^{1/3}$ is the nuclear radius where $r_0 = 1.25$ fm and *A* is the atomic mass number.

It is interesting to examine the consequences of the radial effective Woods-Saxon potential, $V_{WS}\left(r^*\right)$, by using both real and imaginary terms in experiments such as scattering events. We do so in the following section, where we include the Coulomb interaction potential $V_C\left(r\right)$. The total radial effective potential used is

$$V\left(r\right) = V_C\left(r\right) + V_{WS}\left(r^*\right), \tag{2}$$

$$V\left(r\right) = \frac{1.44 Z_{1,2}}{r} - \frac{V_0}{1+\exp\left(\frac{r^* - R_1}{a_1}\right)} - \frac{iW_0}{1+\exp\left(\frac{r^* - R_2}{a_2}\right)}. \tag{3}$$

In Figure 1, we show the real and imaginary parts of the Woods-Saxon potential.

2.2. The Schrödinger Equation with the Woods-Saxon Potential

In this section we solve the radial Schrödinger equation using the radial potential (Equation (3)). The Schrödinger equation is,

$$\left[-\frac{\hbar^2}{2\mu}\nabla^2 + V\left(r\right)\right]\Psi\left(\boldsymbol{r}\right) = E\Psi\left(\boldsymbol{r}\right), \tag{4}$$

where $\mu = \frac{m_1 m_2}{m_1 + m_2}$ is the reduced mass for a two-particle system, *E* is the energy and $V\left(r\right)$ is the radial effective potential calculated in the previous section.

We introduce $U\left(r\right)$, where

$$\Psi\left(\boldsymbol{r}\right) = \Psi\left(r\right) = \frac{U\left(r\right)}{r}, \tag{5}$$

and the Schrödinger Equation (4) is solved by the method of separation of variables. For the radial component we obtain

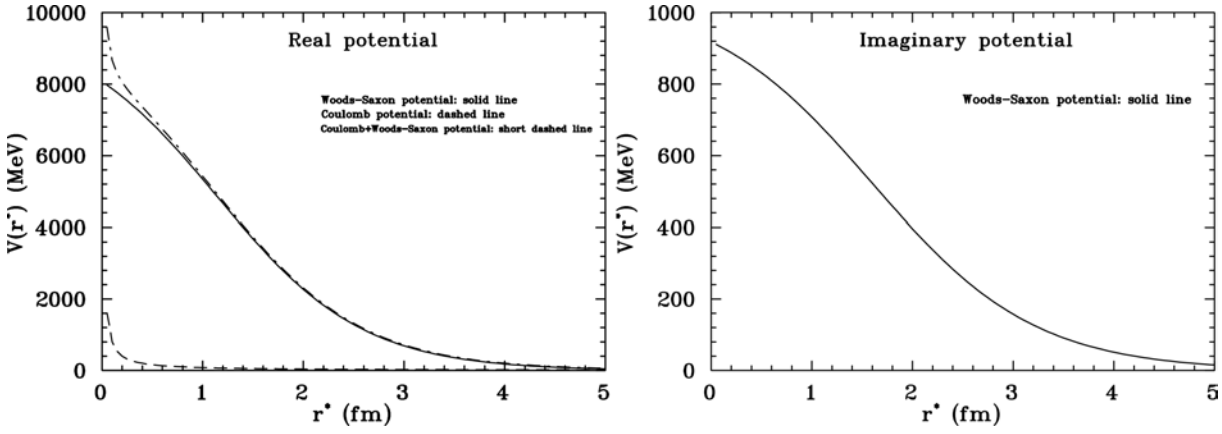

Figure 1. The solid line is for the Woods-Saxon potential using the parameters obtained from the Colorado group (Table I-a from Ref. [2]) and the dashed line is for the Coulomb potential.

$$U_l''(r)+\frac{2\mu}{\hbar^2}\left[E-V(r)\right]U_l(r)-\frac{l(l+1)}{r^2}U_l(r)=0. \tag{6}$$

The radial equation takes the final form,

$$U_l''(r)+\frac{2\mu}{\hbar^2}\left[E-\frac{1.44Z_{1,2}}{r}+\frac{V_0}{1+\exp\left(\frac{r^*-R_1}{a_1}\right)}+\frac{iW_0}{1+\exp\left(\frac{r^*-R_2}{a_2}\right)}\right]U_l(r) \tag{7}$$
$$-\frac{l(l+1)}{r^2}U_l(r)=0.$$

The next step is to determine the set of the parameters for the Woods-Saxon potential. In the Table 1 and Table 2 we show the parameters obtained by minimizing the chi squared value,

$$\chi^2=\sum_{i=1}^{N}\left[\frac{\sigma_{th}(\theta_i)-\sigma_{exp}(\theta_i)}{\Delta\sigma_{exp}(\theta_i)}\right]^2. \tag{8}$$

The calculations for this analysis were done using the experimental data from Fujisawa *et al.* [2].

In Table 1 and Table 2 we show the parameters obtained by minimizing chi squared and using the experimental data from Fujisawa *et al.* [2].

The numerical techniques necessary to solve the Schrödinger equation with a radial potential are explained in chapter 3, Equation (3.28) of Ref. [6]. The solutions of U_l from Equation (7) are introduced in the S matrix (Eq. 10.58 of Ref. [6]), which is,

$$S_l=\frac{U_l(r_{n-1})r_n h_l^-(kr_n)-U_l(r_n)r_{n-1}h_l^-(kr_{n-1})}{U_l(r_n)r_{n-1}h_l^+(kr_{n-1})-U_l(r_{n-1})r_n h_l^+(kr_n)}, \tag{9}$$

where the S matrix is evaluated in the last two points on a mesh of size δ ($r=0,\delta,2\delta,\cdots,n\delta$). U_l are the solutions to the Schrödinger equation with the potential previously calculated and h_l are the spherical Hankel functions defined in Eq. 10.52 of Ref. [6]. The scattering amplitude for a *partial wave decomposition* in terms of the S matrix is,

$$f(\theta)=\frac{1}{2ik}\sum_{l=0}^{\infty}(2l+1)P_l(\cos\theta)(S_l-1). \tag{10}$$

For states with well defined spin and isospin the elastic and total cross section of nucleon-nucleon scattering into a solid angle element $\mathrm{d}\Omega$ is given by the scattering amplitude $f(\theta)$ of the reaction

$$\frac{\mathrm{d}\sigma}{\mathrm{d}\Omega}=\left|f(\theta)\right|^2, \tag{11}$$

$$\sigma_T=\frac{4\pi}{k}Im\left[f(0^\circ)\right], \tag{12}$$

where k is the center-of-mass momentum and $f(0^\circ)$ is the forward amplitude.

The reaction cross section is defined as the subtraction from the integral of the

elastic cross section from the total cross section,

$$\sigma_R \equiv \frac{2\pi}{k^2}\sum_{\ell=0}^{\infty}(2\ell+1)Re(1-S_\ell)-\int\sigma(\theta)\mathrm{d}\Omega. \tag{13}$$

Doing the integration gives

$$\sigma_R = \frac{2\pi}{k^2}\sum_{\ell=0}^{\infty}(2\ell+1)Re(1-S_\ell)-\frac{\pi}{k^2}\sum_{\ell=0}^{\infty}(2\ell+1)\left[|S_\ell|^2+1-2ReS_\ell\right], \tag{14}$$

$$\sigma_R = \frac{\pi}{k^2}\sum_{\ell=0}^{\infty}(2\ell+1)\left(1-|S_\ell|^2\right). \tag{15}$$

The results from the calculations are shown in the next section.

3. Elastic Cross Section

With the analysis performed, we proceed to evaluate numerically the Equations (11)-(12) and (15). We compare the theoretical results with experimental data for elastic cross sections for elastic scattering of helium by nickel atoms [2]. This comparison is made explicitly in **Figures 2-5**.

In **Figures 2-4** the elastic cross section is analyzed for helium by nickel atoms. We evaluate the elastic cross section at energies from T_{Lab} = 24.15, 27.64 and 34.14 MeV considering the radial effective Woods-Saxon potential and setting the parameters to adjust the experimental points (see **Table 1** and **Table 2**).

In **Figure 5** we show the differential cross section at energies above the Coulomb barrier.

Figure 6 shows the total and reaction cross section for the interaction of helium by nickel atoms. We evaluate the cross sections at energies up to $T_{Lab} = 35$ MeV considering the radial effective Woods-Saxon potential and setting the parameters to adjust the experimental points (see **Table 1**).

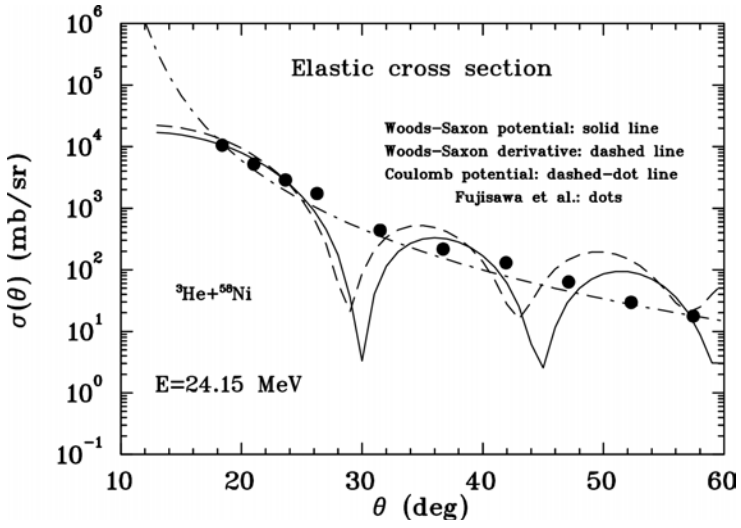

Figure 2. The differential cross section for ^{3}He + ^{58}Ni is plotted as a function of the angle at the energy of 24.15 MeV. The solid line is for the Woods-Saxon potential, the dashed line is with the derivative in the complex term for the Woods-Saxon potential, and the dashed-dot line is for the Coulomb potential. The experimental points come from [2].

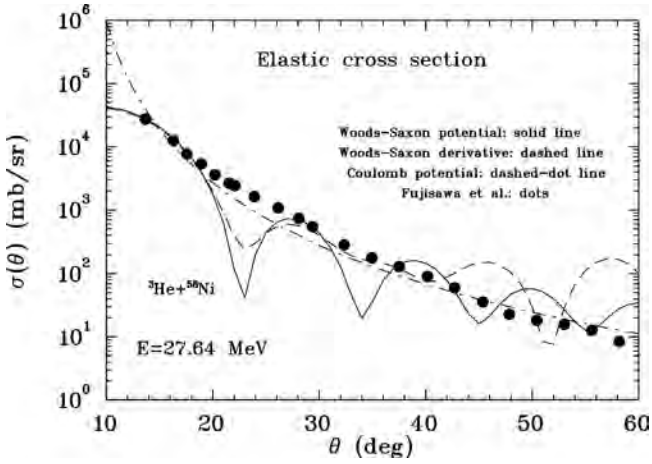

Figure 3. The differential cross section for ^{3}He + ^{58}Ni is plotted as a function of the angle at the energy of 27.64 MeV. The lines and the experimental points have the same meaning as in **Figure 2**.

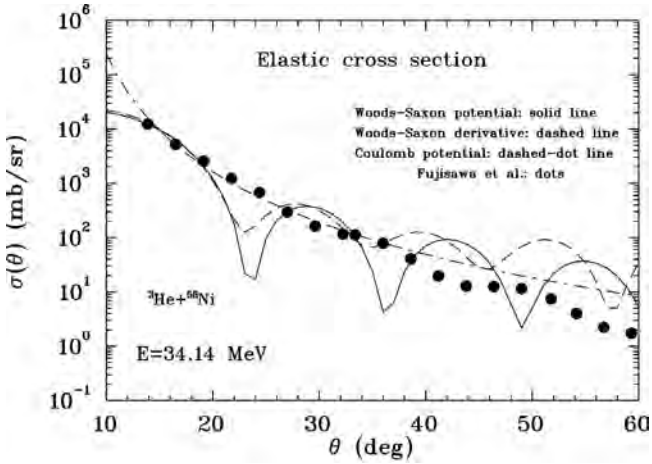

Figure 4. The differential cross section for ^{3}He + ^{58}Ni is plotted as a function of the angle at the energy of 34.14 MeV. The lines and the experimental points have the same meaning as in **Figure 2**.

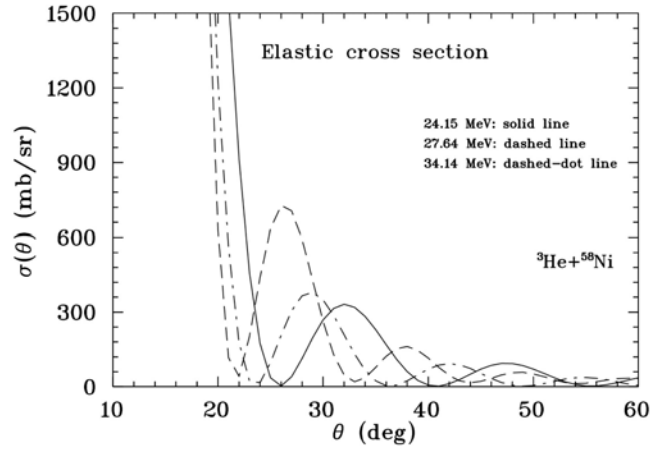

Figure 5. ^{3}He + ^{58}Ni elastic scattering for energies at the barrier Coulomb plotted as a function of the angular distribution. The lines are for the case of a Woods-Saxon potential.

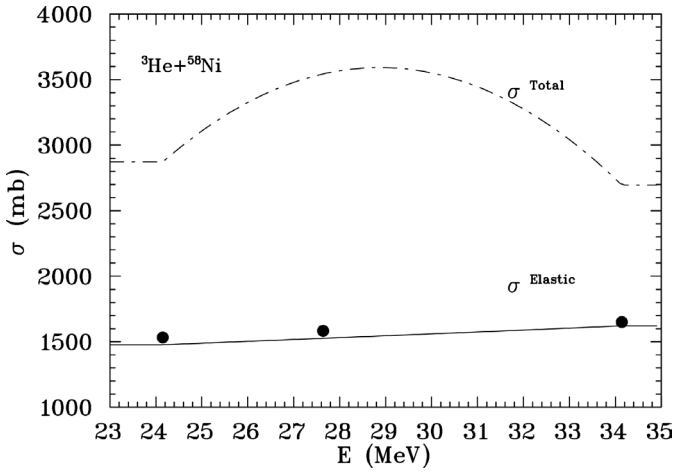

Figure 6. The total and integrated elastic scattering cross section for ^{3}He + ^{58}Ni are plotted as a function of the incident energy. The experimental points come from [2].

4. Conclusions

In this work, we present a numerical solution of the radial Schrödinger equation using a Woods-Saxon potential. We have examined the scattering of helium atoms via nickel. The scattered from alpha particles via nickel atoms was performed and the use of an imaginary term in the Woods-Saxon potential gives a better fit to the experimental data. The parameters for the Woods-Saxon potential were varied until χ^2 was minimized and they are shown in **Table 1** and **Table 2**. The values obtained are better in comparison to those of the Colorado group (Table I-a from Ref. [2]) at the energies of 24.15, 27.64 and 34.14 MeV.

Finally, the total cross section and integrated elastic scattering cross section are calculated and compared with experimental data. We obtain excellent agreement with the experimental data of Fujisawa *et al.* (Ref. [2]) for the set of parameters obtained in **Table 1** and **Table 2**.

Acknowledgements

This work was partially supported by FCFM-UNACH. R. Arceo acknowledges the support of the PFCE 2018.

Conflicts of Interest

The authors declare no conflicts of interest regarding the publication of this paper.

References

[1] Woods, R.D. and Saxon, D.S. (1954) Diffuse Surface Optical Model for Nucleon-Nuclei Scattering. *Physical Review*, **95**, 577-578. https://doi.org/10.1103/PhysRev.95.577

[2] Fujisawa, T., Kamitsubo, H., Wada, T. and Igarashi, M. (1969) Optical-Model Analysis of Elastic Scattering of ^{3}He Particles from ^{58}Ni at 24.15, 27.64 and 34.14 MeV. *Journal of the Physical Society of Japan*, **27**, 278-290.

https://doi.org/10.1143/JPSJ.27.278

[3] Jansen, R.H.J., de Heer, F.J., Luyken, H.J., van Wingerden, B. and Blaauw, H.J. (1976) Absolute Differential Cross Sections for Elastic Scattering of Electrons by Helium, Neon, Argon and Molecular Nitrogen. *Journal of Physics B*, **9**, 185-212. https://doi.org/10.1088/0022-3700/9/2/009

[4] Baron, N., Leonard, R.F. and Stewart, W.M. (1971) Alpha-Gamma Angular Correlations in ^{12}C, ^{24}Mg, ^{58}Ni, and ^{120}Sn. *Physical Review C*, **4**, 1159-1173. https://doi.org/10.1103/PhysRevC.4.1159

[5] Albinski, J., Budzanowski, A., Dabrowski, H., Rogalska, Z., Wiktor, S., Rebel, H., Srivastava, D.K., Alderliesten, C., Bojowald, J., Oelert, W., Mayer-Böricke, C. and Turek, P. (1985) α-Particle Scattering from Ni Isotopes at E_α = 172.5 MeV. *Nuclear Physics A*, **445**, 477-494. https://doi.org/10.1016/0375-9474(85)90453-1

[6] Gibbs, W.R. (2006) Computation in Modern Physics. 3rd Edition, World Scientific Publishing, Singapore.

World Journal of Nuclear Science and Technology, 2020, 10, 9-22
https://www.scirp.org/journal/wjnst
ISSN Online: 2161-6809
ISSN Print: 2161-6795

Design and Analysis of a Metallic Uranium Reactor Type-Pump Using the Magnesiothermy Process

Munir Dides, José Hernández*, Luis Olivares

Chilean Nuclear Energy Commission (CChEN), Santiago, Chile
Email: Munir.dides@cchen.cl, *Jose.hernandez@cchen.cl, Luis.olivares@cchen.cl

How to cite this paper: Dides, M., Hernández, J. and Olivares, L. (2020) Design and Analysis of a Metallic Uranium Reactor Type-Pump Using the Magnesiothermy Process. *World Journal of Nuclear Science and Technology*, **10**, 9-22.
https://doi.org/10.4236/wjnst.2020.101002

Received: September 18, 2019
Accepted: November 19, 2019
Published: November 22, 2019

Copyright © 2020 by author(s) and Scientific Research Publishing Inc.
This work is licensed under the Creative Commons Attribution International License (CC BY 4.0).
http://creativecommons.org/licenses/by/4.0/
Open Access

Abstract

This paper shows a methodology to obtain metallic uranium through a magnesiothermy process. Chile has two experimental reactors operated by the "Chilean Nuclear Energy Commission" (CCHEN). One is 5 MW and the other is 10 MW. In order to fulfill international agreements about nuclear energy for testing purposes of these reactors, CChEN purchased 19.9% enriched uranium hexafluoride, also known as the limit of Low Enriched Uranium (LEU). Due to the capacity of these reactors, they need high-density uranium compounds for their fuel, in order to work with LEU. For this reason, the uranium needs a previous conversion into metallic uranium. The conversion laboratory carried out experiences for reduction of UF_4 with Mg. The main purpose of this study was to analyze the operating conditions under which the reduction reaction takes place, the designed method and the equipment and materials used. The raw material used was dehydrated UF_4, prepared by electrolytic reduction and commercial purity Magnesium. The reaction took place in a cylindrical reactor made of low alloy steel, with a conic section in the lower part. The internal zone was coated with a 2.5 cm thick layer of CaF_2. The process started by applying external heating, according to a heating program, developed specially for this purpose. The reduction reaction took place starting at 650˚C. The result was a cylinder of uranium metal and MgF_2 slag. The crossed cut uranium cylinder showed a smooth and homogeneous surface without inclusions of slag, pores or blisters. The yield of the reaction was of the order of 75% with respect to the expected theoretical value. The uranium cone obtained fulfilled the required conditions for source material for nuclear fuel fabrication, with a uranium content of 97.5%.

Keywords

Magnesiothermy, Metallic Uranium, Heat Balance

1. Introduction

In the decade of the 80s, the Chilean Nuclear Energy Commission (CChEN) bought LEU in form of UF_6. The objective of this purchase was the development of U_3O_8 fuel type compounds for these reactors. However, enrichment reduction international program (RERTR) launched in 1978, affected the continuity of this project, because U_3O_8 uranium compound allows limited uranium load. For this reason, CChEN needed to convert UF_6 (LEU) into metallic uranium, suitable for the manufacture of higher neutron density fuels. This fact allowed using higher density compound, as U_3Si_2. Uranium and silicon form several different stoichiometric compounds including USi_2, USi (or $U_{34}Si_{34.5}$), U_3Si_2, U_3Si [1] [2]. The uranium density and thermophysical properties of high uranium content uranium silicides (U_3Si_2 and U_3Si) make them an attractive material from both an economic and safety point of view as a replacement for UO_2 [3]. Experience from research uranium fuel reactors indicate that U_3Si exhibits too much swelling under irradiation for use as a nuclear fuel. Additionally it decomposes into U_3Si_2 and solid solution U above 900˚C, which is below some expected temperatures in uranium silicide fueled pins. Fortunately, U_3Si_2 has a very promising behavior under irradiation in research reactor fuels and maintains several advantageous properties over UO_2. U_3Si_2 have 17% more uranium atoms in a set volume than in the same volume of UO_2, given a constant percentage of theoretical density for both samples. This superior uranium loading has the potential to enable power uprates, extend cycle length in LWRs, or reduce enrichment, all of which are economically beneficial [4]. This fact raised the need to conduct studies to determine the most favorable conditions, by which uranium metal is prepared.

The literature mentions that the methodology to obtain metallic uranium consists in reducing, by exothermic reaction, UF_4 with a metal, specifically Mg or Ca granules, according to the pre-established operating conditions [5]. This reaction takes place in a closed reactor in an inert atmosphere. The most common method to obtain UF_4 is through the following chemical reactions [6]:

- Direct reduction of UO_3 with H_2 or other organic reducer to obtain UO_2.
- Hydrofluoration of UO_2 in fluidized bed with HF at a temperature between 450˚C and 480˚C.
- Electrolytic reduction of the U^{6+} ions to U^{4+} and its precipitation with F^{1-} ion, or Reduction of the U^{6+} ions with $SnCl_2$.

The remaining methods are feasible to be used to reach UF_4 directly. The hydrolysis reaction of UF_6 that takes place is: [7]

$$UF_6 + 2H_2O = UO_2F_2 + 4HF \quad (1)$$

In the UO_2F_2 compound, the uranium ion has its highest oxidation state valence (U^{6+}). Therefore, a reduction process transforms it into tetravalent uranium (U^{4+}). An electrolysis process or reduction with stannous chloride achieves this process [8]. For this stage of the study, the raw material was uranium tetrafluoride prepared by electrolysis. This method of preparation consists in obtain-

ing a synthetic solution of UO_2F_2 from the solubility of UO_3 depleted with HF. According to the following reaction: [9]

$$UO_3 + 2HF = UO_2F_2 + H_2O \tag{2}$$

The electrolysis process is based on the following ionization reaction:

$$UO_2F_2 = UO_2^{2+} + 2F^- \tag{3}$$

The overall reaction that takes place in the electrolysis cell is as follows:

$$UO_2^{2+} + 2H^+ + 4F^- = UF_4 \cdot \frac{3}{4}H_2O + \frac{1}{4}H_2O + \frac{1}{2}O_2 \tag{4}$$

Or what is the same

$$UO_2F_2 + 2HF = UF_4 \cdot \frac{3}{4}H_2O + \frac{1}{4}H_2O + \frac{1}{2}O_2 \tag{5}$$

Magnesiothermic reduction employs metallic magnesium or calcium as a chemical reducer of uranium. Magnesium is mixed with stoichiometric excess to uranium tetrafluoride (UF_4), according to the following reaction:

$$UF_4 + 2Mg = U + 2MgF_2 \rightarrow \Delta H = -82 \text{ kcal/mol} \tag{6}$$

UF_4 is a greenish substance which, mixed with magnesium, can be reduced to uranium metal under adequate thermal conditions. This reaction is intensely exothermic. The reaction products utilize the resulting exothermic heat and melt to form the uranium ingot at the bottom of the crucible and the slag. The supernatant slag, which contains essentially MgF_2, solidifies at the top of the ingot.

According to other authors, reaction (6) starts at 600˚C - 650˚C [10]. However, this heat generated must be enough to reach the melting reaction products; starting from room temperature, since U melts at 1132˚C and MgF_2 at 1255˚C. To have a proper separation between uranium and slag, the molten products need a viscosity low enough to allow the breakup between them. The Effect of impurities, such as magnesium or uranium oxides, has been found to yield poor slag-metal separation probably due to incomplete reduction and high viscosity of oxide slag [11].

Another important aspect of this process is the presence of humidity and acid coming from the aqueous obtaining process The presence of H_2O or HF leads to evolution of hydrogen by pre-reaction during heating at lower temperatures itself (380˚C - 600˚C), according to the following reactions: [11]

$$Mg + H_2O = MgO + H_2 \tag{7}$$

$$Mg + 2HF = MgF_2 + H_2 \tag{8}$$

$$UO_2F_2 + H_2 = UO_2 + 2HF \tag{9}$$

$$UF_4 + 2H_2O = UO_2 + 4HF \tag{10}$$

$$MgO + 2HF = MgF_2 + H_2 \tag{11}$$

For this reason, it is very important to eliminate both water and acid traces before the beginning of the reaction, along with a preheating of the reactants before the reaction for this process [12].

2. Reactor Design Based on Heat and Mass Balance

The experience of reducing UF_4 with Mg was carried out in a pump-type reactor, which was constructed of low alloy steel, with an effective volume of 30.000 cc. Initially the mass of UF_4 was 4500 g. and the amount of Mg corresponds to the stoichiometric plus 20% excess. The electric oven heated the reactor using an electric oven of 5.5 kW of power. Three resistors distributed the heat, two located on the sides and the third at the bottom. A programmer regulated the power supply and temperature. Figure 1 shows the system used for the experience.

To prevent undesirable oxidation reactions in the dehydrated UF_4-Mg mixture, the powders were contained in an inert atmosphere to remove water from both humidification and crystallization before their use in the process of reduction to metallic uranium. The X-ray diffraction analysis (DRX) of Figure 2 shows that the material used is dehydrated UF_4, with a water level that does not affect the reduction reaction. In this case, the inert gas removed the humidity before the reduction process started.

The UF_4 pellet diameter, about 1.5 to 2 mm, was prepared via an electrolysis of uranyl fluoride (UO_2F_2) solution. The pellets was filtered to obtain the related crystals. The natural moisture from the aqueous obtainment process belongs to the uranium tetrafluoride lattice. To eliminate it, a drying furnace (Figure 3), heated at 150˚C with a ceramic crucible, eliminated the water of crystallization. The Mg was also dried as a precaution for possible adhered moisture.

The final temperature reached by the system once the reaction finished, was calculated based on the specific heat and reaction heats, including heat losses. According to these calculations, the melt temperature should reach 1450˚C. This temperature allowed obtaining a fluid slag, which in turn allows the reduced U

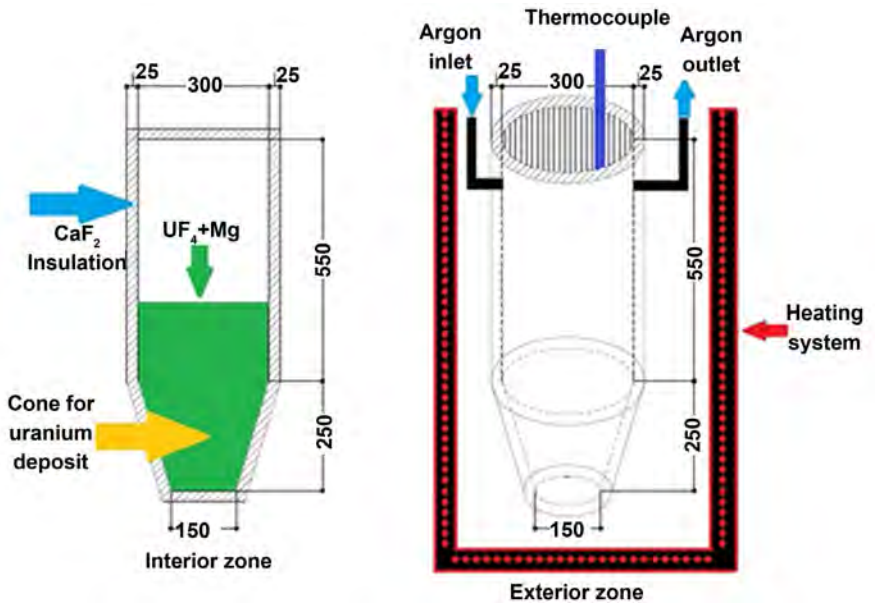

Figure 1. Schematic view of the reactor type pump. Measures in mm.

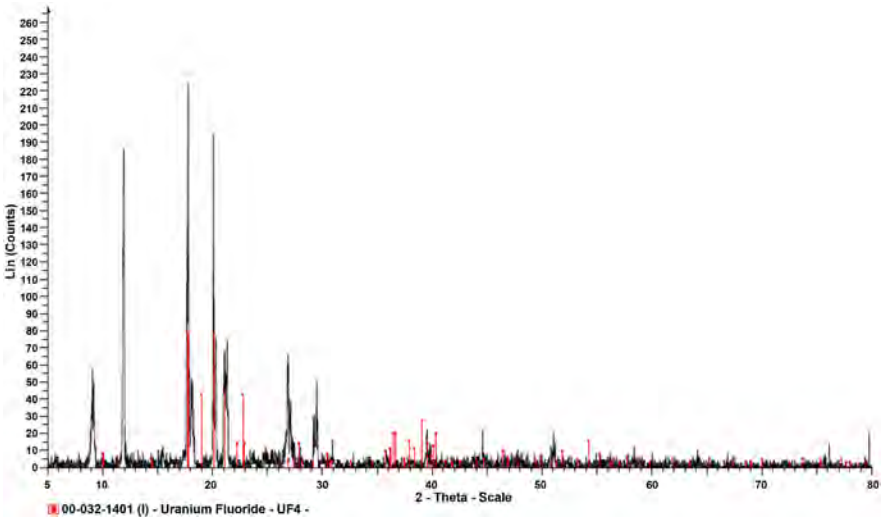

Figure 2. X-Ray Diffraction of the UF_4 compound.

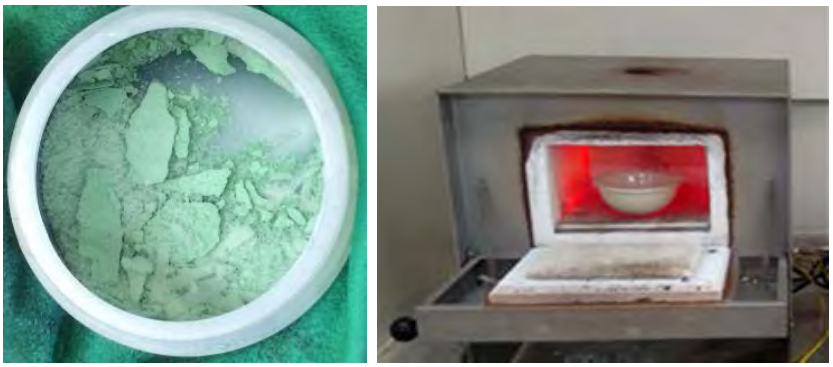

Figure 3. UF_4 crystals sample—Drying furnace.

to decant. The reaction is exothermic and produces 82 kcal per mol formed, once it reaches the indicated temperature.

To determine the degree of preliminary preheating, the reactor needs to achieve the reaction conditions for the spontaneous reaction. The system needs a preliminary thermal balance. **Table 1** shows the values used for the estimation of heat needed for the initial heating. **Table 2** shows the heat requirement for the products obtained by reaction (6).

Table 3 shows the heat generated by reaction (6) and the requirement to melt the products obtained, U + MgF_2, plus the excess heat. This heat is necessary for a good separation of U from the MgF_2 slag.

The reactor at the beginning of the test contained 4500 g of UF_4, equivalent to 12.74 moles. In these conditions, reaction (6) formed 25.48 moles of MgF_2. The temperature expected inside the pump is around 1450˚C. At this temperature, the U formed melts and decant at the bottom of the reactor. The final state of the slag, MgF_2 in this case, and U at this temperature are both liquid. **Table 4** shows estimations for the specific heat of the uranium and the MgF_2 slag, in their molten state.

Table 1. Thermodynamic data used for the heat balance in the final products for the proposed system.

Elements and compounds	Specific heat Cp Cal/g˚C	Sensitive heat. cal/˚C	Melting Heat kcal/g
U	0.028	6.7	4.35
MgF_2	0.238	29.5	13.9
Fe	0.11	3462	-
CaF_2	0.26	2600	-
Mg	0.234	13.6	0.85

Table 2. Heat involved in the reduction reaction (6) per compound.

Uranium = 6.7 Cal/˚C mol
MgF_2 = 29.5 Cal/˚C mol
Total heat = 36.2 Cal/˚C mol
Pump and insulator = 6.06 Kcal/kg˚C

Table 3. Heat produced by reaction (6).

Heat generated by the reaction	Heat to melt $U + 2MgF_2$ + 20% Excess Mg	Sensitive Heat Products $U + 2MgF_2$ + 20% excess	Excess heat
82 Kcal/mol	33 Kcal/mol	6.7 + 29.5 + 2.3 = 38.5 Cal/˚C	49 Kcal

Table 4. Heat available for the molten mixture of $U + MgF_2$.

Heat generated by the reaction (Kcal/mol)	Heat to melt $U + 2MgF_2$ + 20% Excess Mg	Heat available Kcal/mol
90% × 82.0 = 73.8	33 Kcal/mol	40.8 Kcal

However, the balance also considered a yield of 90% for reaction (6). For a 90% UF_4 conversion, the heat available to reach 1450˚C is the following.

Considering this criterion, Table 5 shows the estimation for the specific heat of the molten mixture of $U + MgF_2$ to reach this temperature:

The value of 56.2 Cal/g˚C is the closest estimation for the expected results of this experience. At the proposed temperature, the $U + MgF_2$ mixture has a viscosity low enough to allow the separation during the process.

3. Experimental Development

The trouser mix system of Figure 4 mixed the dried and dehydrated UF_4 product with 20% Mg excess, for 40 min. at 16 R.P.M.

Figure 5 shows the reactor user for the test, including the heating system, the insulation and the argon inlet and outlet:

For insulation inside the reactor, the walls were covered with CaF_2 technical grade, under 180 μm before filling the reactor with the mixture. The density of the compacted mixture is 3 g/cc approximately. With the reactor loaded, the argon cylinder connecting to the pump generates an inert atmosphere to prevent

Table 5. Estimation of the specific heat for U + MgF_2 in molten state.

Heat remaining Kcal	Estimated Cp.m for the mass of U and MgF_2.	Preheating to reach U + MgF_2 melting. ˚C	Temperature difference to reach 1450˚C
40.8	**56.2**	**694**	**756**

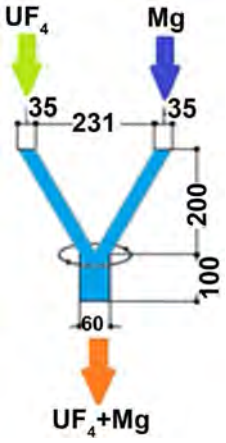

Figure 4. Schematic diagram of the trouser system. Measures in mm.

Figure 5. Magnesiothermy reactor.

the oxidation of the reactants, as undesirable reactions [13]. The argon inside the pump evacuates the air inside. Finally, the argon outlet sent the air to a water column to maintain a positive pressure, equivalent to 1500 mm water column. This positive pressure prevents the entry of gases from the outside. With this pressure achieved, the heating program started through the oven. The reaction started after 16 hrs and at a temperature of 620˚C - 650˚C.

To know the temperature at which the reaction begins, the differential thermal analysis (DTA) from **Figure 6**, determined that the required temperature for the uranium reduction is between 600˚C - 650˚C. Over this temperature, reaction (6) provides the required heat for the reaction.

The noise produced and the temperature increase confirmed the start of the reaction. At this point, the temperature control system shutdown the power

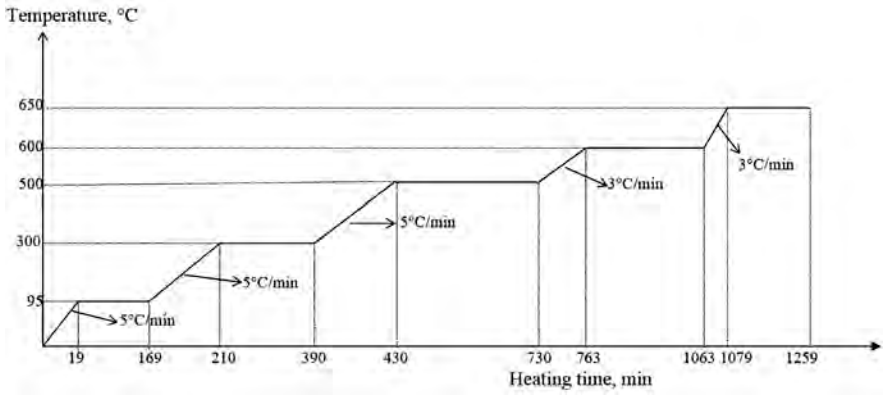

Figure 6. Heating curve for the proposed reactor.

supply to the oven, allowing it to cool freely by natural convection. After 24 hours, the reactor was disassembled and the load removed.

4. Results Obtained

According to the heat and mass balance, the reaction starts when the outside temperature of the oven reaches 650˚C. The proposed system obtains it after 21 hours.

The start of the reaction showed the following phenomenon:

- Heavy noise and vibrations.
- Increased pressure in the reactor pressure gauge and the argon flow regulator. This parameter reached a maximum value of 15 psig.
- Sudden temperature increase, up to the range of 1350˚C - 1400˚C.

Figure 7 shows the start of the pump-type reactor, once the reduction reaction started, at 650˚C:

With this phenomenon detected, the control system turned the oven off and allowed to cool freely until the next day. Table 6 shows the obtained products.

The reaction step lasted 12 hours. At this time, the argon gas flow was stopped because the slag formed in the process prevented the oxidation of the obtained uranium. The cooling was by natural convection, during a period of 16 hours before opening the reactor. The following figures show the aspects observed in the obtained product. Three aspects are highlighted: a porous area within the insulating material, is attributed to gases present during the process that come from moisture not previously removed at the beginning, or decomposition of some loaded product.

Another area corresponds to a dense and compact material immediately after the reactor wall, is CaF_2, used as insulating material.

Figure 8 shows the main product obtain at the end of the process. This figure shows 3 clearly different zones. In the upper part, the Mg-U-slag mixture. The medium zone had the main MgF_2 slag portion. And finally, in the bottom, a uranium billet of high density. The following figures show the main aspects of the obtained products.

Table 6. Products obtained for the process.

Metallic uranium	Slag before grinding	Ground slag	U weight contained in the UF_4 loaded	Operation performance
2582.0 g	2470.0 g	2444.6 g	3410 g.	76%

Figure 7. Magnesiothermy reactor, once the reduction reaction started.

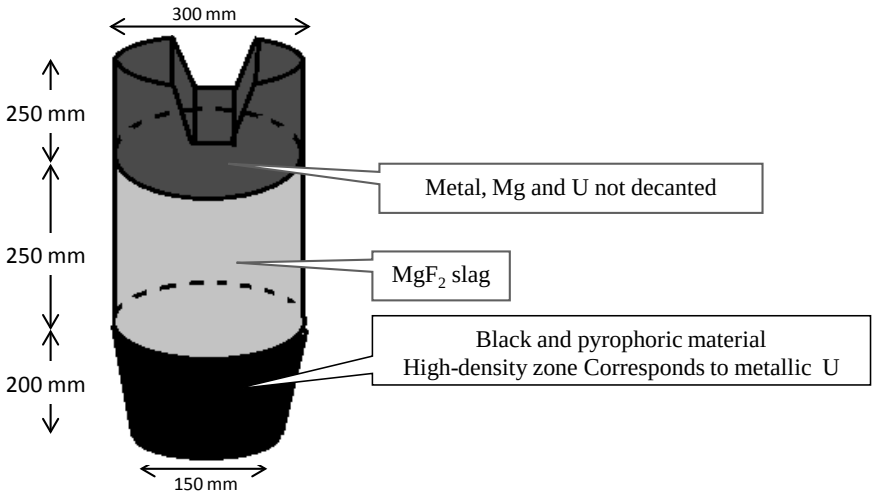

Figure 8. Schematic view of the cross section of the metallic U and the MgF_2 slag.

Figure 9 shows the porous zone inside the insulating material. These zones result in heat losses during the pre-heating and the metallothermic reaction process. This aspect consider the 10% of heat loss during the reduction reaction.

Figure 10 shows the uranium obtained at the bottom of the reactor and the MgF_2 slag at the end of the process. The conic form of the billet allows obtaining a homogeneous final product and the separation from the undesired material. Another important aspect is the empty space during the cooling time. The geometry assured that the contraction suffered by the slag do not reach the uranium billet. In this case, leaving a space of 100 cm. between the slag and the billet.

Figure 11 shows the presence of a portion of metallic uranium during the slag removal. Despite having reached the temperature to reach the molten state, its viscosity was not enough for a correct separation, causing the entrapment inside the slag.

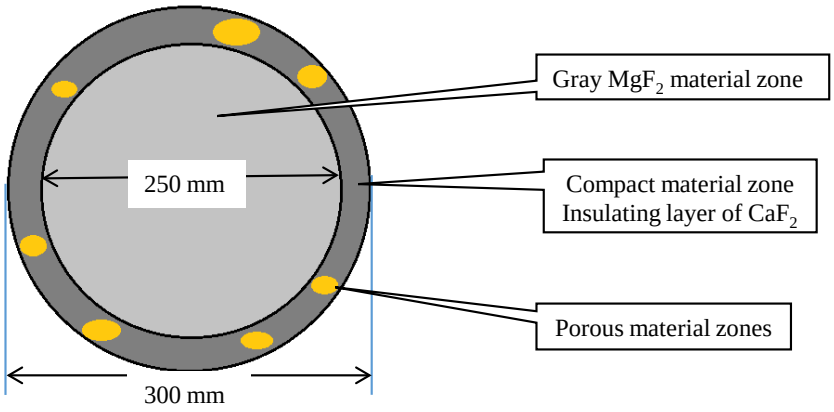

Figure 9. Schematic view from the elevation of the slag and the insulation system.

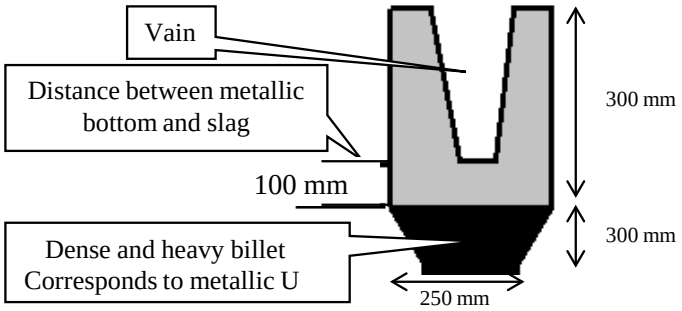

Figure 10. Schematic view of the side of the reactor.

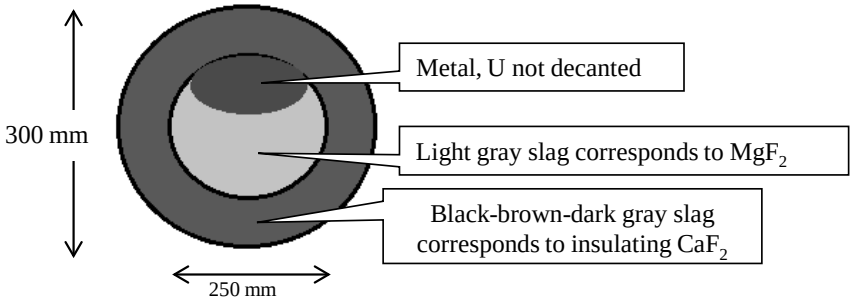

Figure 11. Schematic picture of the superior view of the elevation.

5. Chemical Analysis

Table 7 shows the compositions of the products formed inside the reactor.

Table 8 shows the chemical analysis of the compounds of the reactor and the contamination of every part with residual uranium

Table 8 shows a high uranium content of impurities in the sample coming from the external insulating material. This was because of the high pressure exerted by the energy produced by the reduction reaction. Figure 12 shows disassembly of the reactor and the obtained uranium billet:

It is worth noting that the appearance of the uranium button does not show pores, blisters or inlays inside. This indicates that there was no trapped slag inside the product of interest or the temperature was low at some interior point. It

Table 7. Properties of the obtained products.

Denomination Sample	Origin Material	Properties	DRX Analysis	Differential Thermal Analysis
Sample U CONV-13	Fine insulating CaF_2 material	Easy to grind	CaF_2-SiO_2-UO_2-UF_5 and MgF_2	Weight variation 1.19%
Sample U CONV-14	Insulation material contaminated with black particles	Black particles do not grind easily	CaF_2.-SiO_2.-UO_2 and MgF_2.	No weight loss
Sample U CONV 15	CaF_2 contaminated with black particles	Difficult to disintegrate. it was milled in impact mill	CaF_2.-U_3O_8.-UO_2.-MgF_2.-MgO. Mg. U and Si	It was not subjected to this analysis
Sample U CONV 16	Slag material. MgF_2	Medium hard. grounded with difficulty under 80 mesh	CaF_2.-MgF_2.-UO_2.-MgO.-U.-UF_5. $MgSiO_3$	There is no variation in weight.
Sample U CONV.17	Material of the reactor center. CaF_2.	Easy to grind by contact with the lid	CaF_2. SiO_2. UO_2. $MgSiO_3$ and UF_5	It was not subjected to this analysis

Table 8. Chemical analysis of the obtained products.

Chemical analysis in%	Sample U CONV-13	Sample U CONV 14	Sample U CONV 15	Sample U CONV 16	Sample U CONV 17
U	2.9	0.15	34.0	10.8	0.44
Ca	29.9	33.4	2.56	17.3	38.6
Mg	0.41	0.45	7.1	3.79	0.232
Fe	0	0	0	0	0.15
Si	1.2	3.7	1.1	0	0

Figure 12. Uranium ingot obtained and cross-section of the sample.

presents a smooth, even and uniform fracture that indicates a total fusion and above the melting temperature of the U. This confirms that the system reached the indicated temperature of 1300˚C, according to what the system needs to reach the fusion of the U and its total runoff to the bottom of the reactor. Table 9 shows the chemical composition of the uranium product obtained.

For the reactor tests, the most important impurities in the uranium are boron and cadmium. In this case, the normal content of these impurities should be less than 1 ppm (or μg/g), because of their capacity of neutron absorption during the uranium fuel burning tests. The cadmium and boron levels are appropriate. Other important impurities are oxygen and nitrogen. Their presence was because the insulation conditions were not enough to prevent its oxidation.

The absence of UF_4 in the slag indicates that the reaction was total or in a percentage of the order of 90% to 95%. The X-ray diffraction diagram indicated the presence of UF_5 that may correspond to material trapped in the insulating material. The control of the atmosphere and the overpressure allowed maintaining a constant pressure throughout the experience and prevented most of the oxidation of the initial components. Maintaining the same heating power through time guaranteed a constant temperature profile, with a minimum difference between center and edges. This allowed developing the reaction (6) through the entire reactor. The initial yield of the process achieved a value of 76%. This proves that the system reached the temperatures according to what is needed to reach the fusion of the U to the bottom and the MgF_2 slag to the top of the reactor.

Table 10 shows the experimental results obtained during the experience.

However, Table 11 shows the results using the consideration of a 90% yield for the degree of progress of the reaction:

The difference between the 76% recovery achieved in the billet shown in Figure 5 and the theoretical 90% used for the calculations is because of the uranium trapped in the molten MgF_2 slag and the CaF_2 insulator. In the case of the uranium in MgF_2, this happened because this section did not reached the fusion temperature needed to produce the separation. In the case of the insulator, the uranium was trapped because of the high pressure of reaction (6). According to Table 11, the initial estimation of the specific heat value of 56.2 cal/g˚C for the U + MgF_2 mixture proved to be adequate and adjusted to what happened in the experience

6. Conclusions

The main conclusions of this study are the following:

1) The proposed system allowed obtaining metallic uranium as a final product,

Table 9. Result of the chemical analysis performed on the U obtained.

U %	Zn µ/g	Cd µ/g	Co µ/g	Ni µ/g	Fe µ/g	B µ/g	Mg µ/g	Cu µ/g	Ca µ/g	Al µ/g	O_2 µ/g	N_2 µ/g
97.5	7	<0.1	0.42	26.2	152	0.51	596	52	157	212	214.2	2.523

Table 10. Temperature reached by the solid products.

Remnant heat. cal	Specific heat. Cp	Temperature of the reactants at the beginning of reaction (6)	Temperature immediately after the reaction.
45,700	56.2	620˚C	1433˚C

Table 11. Temperature reached by the solid products, with 90% of reaction efficiency.

Remnant heat. cal	Specific heat. Cp	Temperature of the reactants at the beginning of reaction (6)	Temperature immediately after the reaction.
41,130	61.2	620˚C	1403˚C

with a yield of the order of 76%. The chemical analysis showed a uranium content of 90% - 95% and a level of impurities that allowed producing high-density uranium compounds for Chilean research reactors.

2) The temperature conditions reached allowed the fusion of U and MgF_2 slag. These conditions separated the desired uranium product from the slag. The system achieved temperatures of 1433˚C.

3) The design of the reactor based of thermodynamic considerations of specific heat and latent heat of fusion for the metallic uranium and the MgF_2 slag, for the total mass of the compounds is consistent with the results obtained in the experience.

Conflicts of Interest

The authors declare no conflicts of interest regarding the publication of this paper.

References

[1] Snelgrove, J.L. and Domgala, R.F. (1987) The Use of U3Si2 Dispersed in Aluminum in Plate-Type Fuel Elements for Research and Test Reactors. *ANL/RERTR/TM-11*, Argonne National Lab, IL. https://doi.org/10.2172/5688807

[2] Vaugoyeau, H., Lombard, L. and Morlevat, J. (1972) A Contribution to the Study of the Uranium-Silicon Equilibrium Diagram. *Atomic Energy of Canada Limited*, **39**, 323-329. https://doi.org/10.1016/0022-3115(71)90153-X

[3] Okamoto, H. (1990) Si-U (Silicon-Uranium). de *Binary Alloy Phase Diagrams*, II Ed., T.B. Massalski, 3374-3375.

[4] Harp, J.M., Lessing, P.A. and Hoggan, R.E. (2015) Uranium Silicide Pellet Fabrication by Powder Metallurgy for Accident Tolerant Fuel Evaluation and Irradiation. *Inaho National Laboratory* (*INL*), 1-5. https://doi.org/10.1016/j.jnucmat.2015.06.027

[5] Reilly, D., Athon, M., Corbey, J., Leavy, I., McCoy, K. and Schwantes, J. (2018) Trace Element Migration during UF4 Bomb Reduction: Implications to Metal Fuel Production, Worker Health and Safety, and Nuclear Forensics. *Journal of Nuclear Materials*, **510**, 156-162. https://doi.org/10.1016/j.jnucmat.2018.07.052

[6] Silva Neto, J., Urano de Carvalho, E., Lazzari Garcia, R., Saliba-Silva, A., Gracher Riella, H. and Durazzo, M. (2017) Production of Uranium Tetrafluoride from the Effluent Generated in the Reconversion via Ammonium Uranyl Carbonate. *Nuclear Engineering and Technology*, **40**, 1711-1716. https://doi.org/10.1016/j.net.2017.07.019

[7] Agency, I.A.E. (1994) Properties of UF6 and Other Uranium Compounds. de *Manual on Safe Production*, *Transport*, *Handling and Storage of Uranium Hexafluoride*, IAEA, Vienna, 11-20.

[8] Da Silva Neto, J. (2008) Processo alternativo para obtenção de tetrafluoreto de urânio a partir de efluentes fluorados da etapa de reconversão de urânio. Instituto de pesquisas energéticas e nucleares, Sao Paulo.

[9] Cordfunke, E.H.P. (1969) The Chemistry of Uranium. Elsevier Publishing Company, Petten.

[10] Yemel'Yanov, V.S. and Yevstyukhin, A.I. (2013) The Metallurgy of Nuclear Fuel:

Properties and Principles of the Technology of Uranium, Thorium and Plutonium. Elsevier, Oxford.

[11] Mayekar, S., Singh, H., Meghal, A. and Koppiker, K. (1985) Magnesio-Thermic Reduction of UF4 to Uranium Metal: Plant Operating Experience. Uranium Extraction Division, B.A.R.C., Trombay, Bombay.

[12] Harper, J. and Williams, A. (1957) Factors Influencing the Magnesium Reduction of Uranium Tetrafluoride. *Extraction and Refining of Rarer Metals*, 143-162.

[13] Durazzo, M., Saliba-Silva, A., Martins, I.C., Urano de Carvalho, E.F. and Riella, H.G. (2017) Manufacturing Low Enriched Uranium Metal by Magnesiothermic Reduction of UF4. *Annals of Nuclear Energy*, **110**, 874-885. https://doi.org/10.1016/j.anucene.2017.07.033

World Journal of Nuclear Science and Technology, 2020, 10, 23-31
https://www.scirp.org/journal/wjnst
ISSN Online: 2161-6809
ISSN Print: 2161-6795

A Possible Way to Realize Controlled Nuclear Fusion at Low Temperatures

Shihao Chen[1], Ziwei Chen[2]

[1]Northeast Normal University, Changchun, China
[2]Beijing Jiaotong University, Beijing, China
Email: shchen@nenu.edu.cn, zwchen@bjtu.edu.cn

How to cite this paper: Chen, S.H. and Chen, Z.W. (2020) A Possible Way to Realize Controlled Nuclear Fusion at Low Temperatures. *World Journal of Nuclear Science and Technology*, **10**, 23-31.
https://doi.org/10.4236/wjnst.2020.101003

Received: September 1, 2019
Accepted: November 22, 2019
Published: November 25, 2019

Copyright © 2020 by author(s) and Scientific Research Publishing Inc.
This work is licensed under the Creative Commons Attribution International License (CC BY 4.0).
http://creativecommons.org/licenses/by/4.0/
Open Access

Abstract

This paper presents a new way to realize controlled nuclear fusion. The way is that a single energy neutron beam fuses with given nuclei, such as lithium nuclei or boron nuclei, so that the nuclear energy is released. The sort of fusion can be achieved at low temperatures, because a neutron has no charge and has a large reaction cross section with a nucleus. The fusion is easy to control and does not produce radioactive spent nuclear fuel. One of the five sorts of neutron sources is the electron neutron source in which a single energy electron beam collides with a single energy bare nucleus beam, such as the deuteron, to produce a single energy neutron. These neutrons irradiate target nuclei and are absorbed by the target nuclei, so that nuclear energy is released. Compared with conventional fusion, it has the disadvantage of releasing less energy and energy density. In addition, it takes a certain amount of energy to produce a beam of single-energy neutrons. However, if some of the input energy can be effectively recycled, the fusion process must produce more energy than the input energy.

Keywords

Nuclear Fusion at Low Temperature, Neutron Source, Lithium, Neutron-Rich Nucleus

1. Introduction

So far, controlled nuclear fusion has not realized. That's because not only does fusion need to be hotter than 100 million degrees, but it also needs to satisfy the Lawson conditions. For a 100 million degree plasma, the Lawson conditions are not easy to be satisfied. The fundamental reason is that there is a strong electrostatic repulsive potential between the positively charged bare nuclei. It is ob-

vious that to reduce the nuclear fusion temperature is necessary.

Gamma ray has been produced in many laboratories. A scheme to generate gamma laser has also been proposed [1] [2] [3]. Based on this, [4] has proposed the idea which reduce the fusion temperature by using gamma rays or gamma lasers to irradiate the target nucleus so that the target nuclei are in an excited state. Different from this, this paper considers using neutrons to achieve nuclear fusion. Compared with conventional fusion, it has the disadvantage of releasing less energy and energy density. In addition, a certain amount of energy is required to produce a single-energy neutron beam. In order to output energy is larger than input energy, the thermal energy and light energy generated by the neutron beam generation process need to be effectively recycled. On the plus side, the fusion process can be done at low temperatures, easily controlled and no radioactive spent fuel to be produced.

2. The Physical Mechanism of Controlled Fusion at Low Temperatures

2.1. The Fusion of Neutrons and Nuclei

If the combining mode A of a nucleon system has higher energy than another combining mode B, when the nucleon system changes from A combining mode to B, there must be some nuclear energy to be released. Regardless of nuclear fission, conventionally designed nuclear fusion, or controlled fusion at low temperatures here, the physical principle of nuclear energy release is the same. The principle of controlled fusion at low temperatures is that a single energy neutron beam fuses with given nuclei so that the nuclear energy is released. The sort of fusion can be achieved at low temperatures, because a neutron has no charge and has a large reaction cross section with a nucleus, moreover, neutrons can be produced without protons colliding with nuclei or nuclei colliding with nuclei, so that the entire process of nuclear fusion does not have to overcome the electrostatic potential energy between the nuclei. A neutron can react with almost any nuclear. There are many kinds of nuclei which release nuclear energy after they absorb neutrons. For example,

$$\mathrm{n} + {}^{6}\mathrm{Li} \rightarrow \alpha + {}^{3}\mathrm{T} + 4.78\ \mathrm{MeV}, \quad \sigma_{nLi} = 936b, \tag{1}$$

$$\mathrm{n} + {}^{10}\mathrm{B} \rightarrow \alpha + {}^{7}\mathrm{Li} + 2.792\ \mathrm{MeV}, \quad \sigma_{nB} = 3840b, \tag{2}$$

where σ_{nLi} and σ_{nB} are the inelastic scattering cross sections of a thermal neutron with ^{6}Li and ^{10}B, respectively.

2.2. Neutron Sources

There are the five sorts of neutron sources which are the spallation, the reactor, the spontaneous emission, the electron and the gamma ray neutron sources. The latter three sorts of neutron sources are considered for use in this controlled fusion at low temperatures. The physical mechanism of electron neutron sources is as follow. In a vacuum chamber, neutron-rich atoms are dissociated into electrons and bare nuclei. The electrons and bare nuclei are separated by electric

field and magnetic field according to traditional technology, and are respectively modulated into a single-energy electron beam and a single-energy bare nucleus beam. The directions of the single-energy electron beam and the single-energy bare nucleus beam are opposite from each other. The kinetic energy of the electron relative to the bare nucleus is greater than the binding energy of the last neutron of the bare nucleus. As a result, after the electron collides with the bare nucleus, the neutron-rich bare nucleus will be broken into several daughter nuclei and neutrons due to electromagnetic and weak interactions. The electromagnetic interaction is clearly predominant here. The energies of the released neutrons are different from each other when the velocities of the single-energy electron beam relative to single-energy bare nucleus beam are different. Neutrons can be released out from many sorts of neutron-rich nuclei when electrons collide with the neutron-rich nuclei. For example, there is the following reaction when the kinetic energy of an electron relative to a deuteron is greater than the binding energy of a deuteron 2.224 MeV,

$$\mathrm{e}^- + \mathrm{d} \to \mathrm{e}^- + \mathrm{p} + \mathrm{n} - 2.224\ \mathrm{MeV}, \tag{3}$$

$$\mathrm{e}^- + \mathrm{d} \to \nu_\mathrm{e} + 2\mathrm{n} - 2.224\ \mathrm{MeV}. \tag{4}$$

There is the following reaction when the kinetic energy of an electron relative to the beryllium nucleus ^{9}Be is greater than the binding energy of the last neutron in a ^{9}Be nucleus 1.665 MeV,

$$\mathrm{e}^- + {}^9\mathrm{Be} \to \mathrm{e}^- + {}^8\mathrm{Be} + \mathrm{n} - 1.665\ \mathrm{MeV}, \tag{5}$$

$${}^8\mathrm{Be} \to 2\alpha + 0.092218\mathrm{MeV},\ T\left({}^8\mathrm{Be}\right)/2 = 0.07\ \mathrm{fs}. \tag{6}$$

Analogously, a neutron-rich nucleus can also release neutrons when it absorbs a gamma photon whose energy is greater than the binding energy of the last neutron of the rich nucleus. For example, when the energy of a gamma photon is larger than 2.224 MeV there is the following reaction

$$\gamma + \mathrm{d} \to \mathrm{p} + \mathrm{n}. \tag{7}$$

when the energy of a gamma photon is larger than 1.665 MeV there is the following reaction

$$\gamma + {}^9\mathrm{Be} \to {}^8\mathrm{Be} + \mathrm{n}. \tag{8}$$

Some radioactive elements can release neutrons. The elements can used as the spontaneous emission neutron sources. One of the spontaneous emission neutron sources is ^{252}Cf, its half-life is $T/2 = 2.645a$, its neutron yield is $2.31\times10^{12}\,\mathrm{s}^{-1}\cdot\mathrm{g}^{-1}$, its energy spectrum distribution is the maxwell distribution, $N(E) = C\sqrt{E}\exp\left(-E/E_r\right)$, here $E_r = 1.453 \pm 0.017$ MeV, and C is a normalization constant, in which some neutrons can fuse with the target nuclei ^{6}Li and ^{9}Be. It is obvious that the energies of released neutrons by different radioactive elements are different from each other.

2.3. The Ratio of Nuclear Energy Released to Energy Consumed

To sum up, it can be seen that the process of the fusion of neutrons and nuclei is

as follows. First, a large number of single-energy neutrons need to be produced. Secondly, the single-energy neutrons are fused with the target nucleus. Let the energy really consumed in the first step be E_N, the energy released in the second be E_F, only when $S = E_F / E_N > 1$, the fusion is meaningful.

Let the binding energy of the electrons and the nucleus of a neutron-rich atom be E_A. In order to dissociate this atom into its bare nucleus and its electrons, it is necessary to input the energy $\tilde{E}_A = E_A / \eta_A > E_A$, here η_A is the efficiency of $\tilde{E}_A$. In the final phase, these electrons will recombine with the positive ions to form atoms and to release optical energy E_{AO}. In general, $\Delta E_A = \tilde{E}_A - E_A$ will transform to thermal energy. A part $\eta_{AO} E_{AO}$ of E_{AO} and a part $\eta_a \Delta E_A$ of ΔE_A can be recycled, here $\eta_{AO} < 1$ and $\eta_a < 1$ are the efficiencies of E_{AO} of ΔE_A, respectively. Consequently, the energy actually consumed in the process is $E_{AC} = \tilde{E}_A - \eta_{AO} E_{AO} - \eta_a \Delta E_A$. It is possible $E_{AC} < E_A$.

Let the consumed energy be E_S in the process to modulate electrons into a single-energy electron beam and bare nuclei into a single-energy bare nuclear beam, and the optical energy radiated by the electrons and the bare nuclei be E_{SO} when they accelerate or decelerate in the process. One part of E_S is dedicated to the single electron beam and the single bare nuclear beam, and the remaining part of E_S is E_{SO}. A part of E_{SO} can be recycled, so the actual energy consumed in this process is $E_{SC} = E_S - \eta_{SO} E_{SO}$, here η_{SO} is the recycled efficiency of E_{SO}.

To sum up, it can be seen that the process of the fusion of neutrons and nuclei is as follows. First, dissociate neutron-rich atoms into electrons and bare nuclei. For example, electrolysis of heavy water D_2O yields D_2. Dissociation of the heavy hydrogen gives the deuterons and electrons. Secondly, to modulate the electrons into a single-energy electron beam and neutron-rich nuclei into a single-energy bare beam. The kinetic energy of the electron in the beam relative to the bare nucleus is greater than the binding energy of the last neutron of the bare nucleus. Thirdly, in the colliding zone, the single-energy electron beam collides with the single-energy bare nuclear beam. As a result, single-energy neutrons are released, such as the process described in (3). Fourthly, the single-energy neutrons irradiates the given target nuclei and fuse with the target nuclei. The target nuclei disintegrate and releases nuclear energy, such as the process described in (1)-(2).

Let the energy of the initial state of a nuclear system be E_I, and the energy of the final state be E_F, $E_{IF} = E_I - E_F$ is the energy released by the nuclear system when it transforms from the initial state to the final state. But this energy cannot be released directly. It is necessary to go through an intermediate process. Let the energy required to transform from this initial state to this final state be E_M. In this case, the energy difference between the initial state and the final state is still the same, *i.e.* $E_{IF} = (E_I + E_M) - (E_F + E_M)$. One part $E_{MN} = \eta_N E_M$ of E_M is used to release neutrons and transformed into kinetic energy of the single-energy neutrons, while the remaining part $E_{MT} = \eta_T E_M$ of E_M is transformed into heat and light energy. One part $E_{MTR} = \eta_{TR} E_{MT}$ of E_{MT} can be re-

cycled, and the remaining part $E_{MTD} = \eta_{TD} E_{MT} = E_{MT} - E_{MTR}$ of E_{MT} is dissipated. To sum up, it can be seen that if the output energy E_{IF} of this fusion process is greater than the dissipated energy, *i.e.* $E_{IF} > E_{MTD}$, $E_{FD} = E_{IF} - E_{MTD} > 0$ is the net output of energy in the fusion process. If $E_{IF} \le E_{MTD}$, there is no net output of energy. E_{FD} depends on the specific technology of recycling. There possibly is net output of energy in the fusion of neutrons and nuclei.

For example, let the initial state be composed of a deuteron d and a lithium nucleus ^{6}Li, the final state be composed of α, p and ^{3}T, the energy difference between the initial state and the final state is

$$\begin{aligned}&\left[\left(m_d + m_{Li}\right) - \left(m_\alpha + m_T + m_p\right)\right]c^2\\ &= \left[\left(2.14102 + 6.015123\right) - \left(4.002603 + 3.016050 + 1.007825\right)\right] \times 931.49432\\ &= 2.558815 \text{ MeV}.\end{aligned} \quad (9)$$

This initial state of course can not be directly transformed to this final state. In order to realize this transformation the following intermediate physical processes are necessary. Deuterium molecules D_2 are dissociated into electrons and deuterons. The electrons and the deuterons are modulated into single energy electron beam and single energy deuteron beam, respectively. The kinetic energy of an electron in the electron beam relative to the deuteron beam is greater than 2.224 MeV. The electron beam collides with the deuteron beam in the collision zone, so that single energy neutrons are released. The neutrons irradiate the target nuclei ^{6}Li and fuse the nuclei ^{6}Li. Thus, the initial state ($d + {}^6\text{Li}$) transforms into the final state ($\alpha + {}^3\text{T} + \text{p}$) by the immediate state ($\text{p} + \text{n} + {}^6\text{Li}$). The energy released in the transformation from the immediate state to the final state is

$$\begin{aligned}&\left[\left(m_p + m_n + m_{Li}\right) - \left(m_\alpha + m_T + m_p\right)\right]c^2\\ &= \left[\left(1.007825 + 1.008665 + 6.015123\right) - \left(4.002603 + 3.016050 + 1.007825\right)\right]\\ &\quad \times 931.49432\\ &\simeq 4.783 = \left(2.224 + 2.559\right)\text{MeV}.\end{aligned} \quad (10)$$

In order to obtain thermal neutrons with single energy from D_2O, the input energy must be larger than the binding energy of deuteron. On the other hand, not all thermal neutrons can fuse with lithium nuclei. Therefore, the inputting energy for releasing a thermal neutron must be significantly larger than the binding energy of the deuteron. But as long as the recycling technology is good, there must be $E_{IF} > E_{MTD}$.

There is no fusion of protons and nuclei or nuclei and nuclei in the whole process, hence this fusion of neutrons and nuclei can realized at low temperatures. In principle it can be done at room temperature.

The velocities of single-energy electron beam and single-energy deuteron beam in the laboratory coordinate system are v_e and v_d, respectively, and their directions are opposite from each other, Thus the velocity of electrons relative to the deuterons is

$$u_{ed} = \frac{v_e + v_d}{1 + v_e v_d / c^2}.$$

when the electron's kinetic energy relative to the deuteron is greater than 2.224 MeV, $u_{ed} \geq 0.983c$. In order to reduce energy dissipation, $v_d \leq 30$ m/s is taken. So $u_{ed} \simeq v_e$ and $v_d / v_e \leq 10^{-7}$.

Let n_d be the number density of the deuteron in the laboratory, and in the case the inelastic scattering cross section of electron and deuteron be $\sigma_{ed0} = \sigma_{ed0}(\mathrm{e} + \mathrm{d} \to \mathrm{p} + \mathrm{n})$, and the length of the collision zone of electron and deuteron be L_{ed}, then when

$$\sigma_{ed0} n_d L_{ed} = 1, \tag{11}$$

$$n_e v_e = n_d v_d, \quad n_d = 1/\sigma_{ed0} L_{ed} = 10^7 n_e, \tag{12}$$

the inelastic scattering probability of each incident electron with the deuteron is close to 1. When L_{ed} is very large, $\tilde{L}_{ed} = L_{ed}/k$ can been taken as the length of the collision zone, here k is an integer. In this case, some electrons have no inelastic scattering with the deuteron. The electrons will be again transported into a speed regulating device, and then are transported back to the collision zone. In this process, these electrons are in accelerated motion and radiate light. This light, especially synchrotron radiation, can be recycled.

Let the cross section of single-energy deuteron beam be S, which is also the cross section of single-energy electron beam, then the deuteron current intensity and electron beam current intensity are respectively

$$J_d = e^+ n_d v_d S = -e^- n_e v_e S = -J_e \tag{13}$$

A deuteron can release a neutron when it absorbs a photon with its energy to be larger than the bind energy of a deuteron 2.224 MeV. Thus, single energy neutrons can be obtained by gamma laser or single energy gamma photon beam to irradiate the deuterons. Let the inelastic scattering section of a such gamma photon with a deuteron be $\sigma_{\gamma d}$, then when

$$\sigma_{\gamma d} n_d L_{\gamma d} = 1, \tag{14}$$

$$n_d v_d = n_\gamma c, v_d \leq 30 \text{ m/s}, n_d \geq 10^7 n_\gamma, \tag{15}$$

where $L_{\gamma d}$ is the length of the collision zone of the gamma photons with the deuterons, and n_γ is the number density of the gamma photons, the probability of each gamma photon being absorbed by the deuterons is close to 1.

Using these single-energy neutrons to irradiate lithium or boron atoms, fusion reactions (1) or (2) will occur. Let the number density of ^{6}Li nuclei and ^{10}B nuclei be n_{Li} and n_B. lithium or boron atoms are placed in the annular cylinder around this thermal neutron source. The radius differences between the inner and outer cylinders are L_{Li} and L_B, respectively, when

$$\sigma_{nLi} n_{Li} L_{Li} = 1, \ \sigma_{nB} n_B L_B = 1, \tag{16}$$

The probability of each neutron to be absorbed of is close to 1.

The binding energy of a deuterium is less 14 eV. Therefore, in the process of

making a single energy electron beam and a single energy deuteron beam, the average actual energy dissipation of one deuteron and one electron is not more than 1 KeV. It can be seen from the above that if the probability of absorption of a single energy electron by deuterons is greater than 0.7, and the probability of absorption of a single energy neutron by lithium atoms is greater than 0.9, then the average net energy gained from the fusion process of one deuterium and one lithium is greater than 1 MeV.

3. A Device for Fusion of Neutrons with Nuclei

This fusion device consists mainly of the following parts. A vacuum colliding zone of a single energy electron beam with a single energy nucleus beam composed of neutron-rich bare nuclei, the input and output channels of electrons, the input and output channels of neutron rich nuclei, a device dissociating neutron-rich atoms into the electrons and the neutron-rich nuclei, a device of modulating electronic velocities, a device modulating velocities of neutron-rich nuclei, a target atom container T, the channels of the target atoms to be imported into T and to be out exported from T, a device separating ions, electrons and target atoms, and energy transfer device.

The colliding zone is a cylinder C, which is parallel to the X-axis, with a length of L and a diameter of r, two open ends, and surrounded by thin walls which can withstand high temperature and allow neutrons to pass through smoothly. Electric and magnetic fields parallel to the X-axis are distributed in the colliding zone .In the colliding region C, the single energy electron beam collides with the single energy neutron-rich nuclear beam, so that single energy neutrons are released. Here the kinetic energy of an electron relative to the neutron-rich nucleus is greater than the final binding energy of the neutron in the rich nucleus.

The target atoms container T is composed of an outer cylinder, an inner cylinder and two sides. The outer cylinder is a cylinder with radius R, length L and coaxial line with the colliding zone C, made of lead plate absorbing neutrons. The inner cylinder is just cylinder C. The container T is filled with target atoms whose nuclei will fuse with neutrons. The two sides of the container T connect the pipe importing the target atoms into T and the pipe exporting the target atoms from T, respectively.

The target atoms flow into the container T at the required velocity v through the inlet of the container T, and flows out of the container T at the same velocity v through the outlet. The target atoms which have absorbed the neutrons break into several daughter nuclei and electrons. These particles flow out of the container T and then flow into the separation device of the ions, electrons and target atoms in which there is a given magnetic field. Under the action of the magnetic field, these daughter nuclei and electrons are respectively concentrated to form the positive and negative poles of the power. The target atoms which doesn't absorb the neutrons are again transported to the container T.

At both ends of the colliding zone C along the Y direction there are electron importing and exporting pipelines and the importing pipelines of neutron-rich

nuclei, respectively. There is magnetic field in the z direction of the pipelines. Under the magnetic field, the daughter nuclei are separated and then recombined with the electrons to form atoms and to release energy. The atoms are collected after cooling.

Under action of the magnetic field, the neutron-rich nuclei without absorbing neutrons are separated and then input into the velocity modulation device of neutron-rich nuclei. Under action of the magnetic field, the electrons are separated and then input into the electron velocity modulating device.

There are the given electronic field and magnetic field in the electronic velocity modulating device. The electrons are decomposed into multiple beams according to the velocities of the electrons. Then electrons with different velocities are modulated into the same single-energy electron beam. The same is true for the velocity modulating device of neutron-rich nuclei. The device dissociating neutron-rich atoms dissociates neutron-rich atoms into bare nuclei and electrons. The electrons and the neutron-rich bare nuclei are transported to the electron velocity modulating device and the velocity modulating device of neutron-rich nuclei, respectively.

The single energy electron beam and the single energy beam of neutron-rich nuclei are imported into the colliding zone, respectively.

The energy transmission system absorbs and transmits the energy released by fusion and the heat and the light energy converted from the input energy.

4. Conclusion

The mechanism of this sort of controlled nuclear fusion is that single energy neutrons fuse with given nuclei, such as ^{6}Li or ^{10}B, to release nuclear energy. One of the five types of neutron sources is the electron neutron source, where a single energy electron beam collides with a single energy bare nuclear beam (such as deuterium) to produce a single energy neutrons. These neutrons irradiate the target nucleus and are absorbed by the target nucleus so that nuclear energy is released. Compared with conventional nuclear fusion, it has the disadvantages of low energy release and low energy density. In addition, it takes a certain amount of energy to produce a beam of single-energy neutrons. However, if some of the input energy can be effectively recycled, the fusion process must produce more energy than the input energy. On the plus side, this fusion process can be done at low temperatures (in principle, at room temperature), because a neutron has no charge and has a very large cross section with nuclei. The fusion is easy to control and does not produce radioactive spent nuclear fuel.

Acknowledgements

This work is supported by National Natural Science foundation of China 11075064. We are very grateful for the fund's support.

Conflicts of Interest

The authors declare no conflicts of interest regarding the publication of this paper.

References

[1] Chen, S.H. and Chen, Z. (2014) Electron-Photon Backscattering Laser. *Laser Physics*, **24**, 045805. https://doi.org/10.1088/1054-660X/24/4/045805

[2] Chen, Z. and Chen, S.H. (2015) A Discussion on Electron-Photon Backscattering Lasers and Electron-Photon Backscattering Laser in a Laser Standing Wave Cavity. *Laser Physics*, **4**, 045803. https://doi.org/10.1088/1054-660X/25/4/045803

[3] Chen, S.H. and Chen, Z. (2016) Coherent Conditions of Electron-Photon Backscattering Light in a Wiggle Magnetic Field. *Laser Physics*, **26**, 025807. https://doi.org/10.1088/1054-660X/26/2/025807

[4] Chen, S.H. and Chen, Z. (2018) A Way to Realize Controlled Nuclear Fusion by γ-Laser or γ-Ray. *World Journal of Nuclear Science and Technology*, **8**, 190-196. https://doi.org/10.4236/wjnst.2018.84016

World Journal of Nuclear Science and Technology, 2020, 10, 32-38
https://www.scirp.org/journal/wjnst
ISSN Online: 2161-6809
ISSN Print: 2161-6795

Isobars Separation (^{137}Cs-^{137m}Ba-^{137}Ba) from Marine Sediments, in Order to Evaluate Directly Their Radioactive Contamination by Mass Spectrometry

Karla Fernández, Juan Manuel Navarrete, Miguel Angel Zúñiga, Ernesto Hernández

Department of Inorganic and Nuclear Chemistry, Faculty of Chemistry, National Autonomous University of Mexico, Mexico City, Mexico

Email: jmnat33@unam.mx

How to cite this paper: Fernández, K., Navarrete, J.M., Zúñiga, M.A. and Hernández, E. (2020) Isobars Separation (^{137}Cs-^{137m}Ba-^{137}Ba) from Marine Sediments, in Order to Evaluate Directly Their Radioactive Contamination by Mass Spectrometry. *World Journal of Nuclear Science and Technology*, **10**, 32-38.
https://doi.org/10.4236/wjnst.2020.101004

Received: October 5, 2019
Accepted: November 26, 2019
Published: November 29, 2019

Copyright © 2020 by author(s) and Scientific Research Publishing Inc.
This work is licensed under the Creative Commons Attribution International License (CC BY 4.0).
http://creativecommons.org/licenses/by/4.0/

Open Access

Abstract

Marine sediments contamination by fission product ^{137}Cs-^{137m}Ba is a fact since the period 1945-65, when plus than two thousand atomic explosion tests were performed mainly in the southern seas, earth region with minor population density. However, marine flows have produced dissemination of this radioactive pair through the sea bottom all over the world, at different levels, because the sea movement and natural decaying of radioactive pair: parent ^{137}Cs ($t_{1/2}$ = 30.17 years) and daughter ^{137m}Ba ($t_{1/2}$ = 2.55 minutes). Radioactive detection of these contaminants, compared as percentage with that of natural ^{40}K ($t_{1/2}$ = 1.28×10^9 years, 0.0118% of elementary K) leads to radiation contamination factor (RCF), as one possible unit to measure the radioactive contamination intensity in different regions, as well to determine if there is some other possible source of this contaminant, for example water cooling from power nuclear reactors when it is discharged at sea. However, radioactive detection always implies an unavoidable statistical variation, which makes more difficult to appreciate the changes as function of time and region. But at beginning of this century, mass spectrometry has got impressive advances, which makes it much more precise and sensible than radioactive detection [1]. This paper attempts to measure with other units the radioactive contamination: ^{137}Cs atoms number per gram of sample, instead radioactivity, which could be more direct and with minor standard deviation that radioactive detection, solving at same time the isobars separation: ^{137}Cs versus ^{137m}Ba plus elementary ^{137}Ba (11.23% of Ba element).

Keywords

Isobars, Separation, ^{137}Cs-^{137m}Ba-^{137}Ba

1. Introduction

Till now, Radioactive Contamination Factor (RCF) has been established by radioactive detection of contaminant product ^{137}Cs-^{137m}Ba, present in marine sediments, in order to compare it with ^{40}K natural radioactivity as a percentage [2] [3]. This procedure requires to set up about half kilogram of conditioned dry sample in a Marinelli container to be detected either by a NaI(Tl) low background detector during 8 - 12 hours, or to be detected longer time by a HPGe detector. Efficiencies of these procedures have been about 5.6% for ^{137}Cs and 2.9% for ^{40}K in NaI(Tl) scintillation detector, and 0.47% for ^{137}Cs and 0.25% for ^{40}K, in HPGe detector, basic figures to obtain the RCF, in spite of some high statistical variation, even when detection times were as large as possible. So, this paper describes how one cation exchanger resin allows separating isobars from IA and IIA columns of Periodic Table, corresponding to alkaline and earthy-alkaline metals, to establish only atoms number of radioactive contaminant ^{137}Cs-^{137m}Ba. In order to obtain this result by Inductively Coupled Plasma-Mass Spectrometry (ICP-MS), it becomes necessary the previous separation of natural isotope ^{137}Ba (11.23% of natural Ba), to count only ^{137}Cs-^{137m}Ba atoms with much lower statistical variation than that of radioactive detection.

2. Experimental

As cation exchanger was used AMP-PAN cesium resin, ammonium molybdophosphate (AMP), embedded in an organic matrix of polyacrylnitrile (PAN), produced by Triskem International Laboratory in Rennes, France (**Figure 1**). Also possible was to elaborate either zirconium antimonate or zirconium vanadate as cation exchangers [4] [5], but the efficiency proof performed with the first one to obtain 97% - 99% in the final basic solution from a ^{137}Cs-^{137m}Ba acid

Figure 1. Triskem International AMP-PAN (ammonium molybdo phosphate embedded in polyacrylnitrile) resin cation exchanger.

solution with known radioactivity was satisfactory enough, obtained by comparing counts per hour from the acid solution and resin after it trapped the radioactive ^{137}Cs from the initial solution (Figure 2), with counts obtained in the final basic solution (97% of ^{137}Cs-^{13m}Ba in solution previously filtrated twice in the resin) (Figure 3). To do it, 1 gram of resin was conditioned in 10 ml of 10^{-5} M HCl, and put in the filtration plastic tube as compacted as possible. Then it was filtered through it 20 ml of solution pH = 1.5 (^{137}Cs-^{137m}Ba, 10 Becquerel). Then the final recovery was performed by 10 ml, 5M NH_4Cl, pH = 9.5 solution. When this basic solution was detected, it was found 97% of counts produced by ^{137}Cs-^{137m}Ba acid solution previously filtered. Nevertheless, it should be considered for this separation, that transient equilibrium established between ^{137}Cs-Ba^{137m} represents one extreme case of different half lives for radioactive parent and daughter, since $t_{1/2}(^{137}\text{Cs})$ = 30.07 years, while $t_{1/2}(^{137m}\text{Ba})$ = 2.55 minutes. As a consequence, the proportion between both decay constants is as great as:

$\lambda_1\left(^{137}\text{Cs}\right) = 0.693/30.07\times365\times24\times60 = 4.385\times10^{-8}\ \text{min}^{-1}$ and

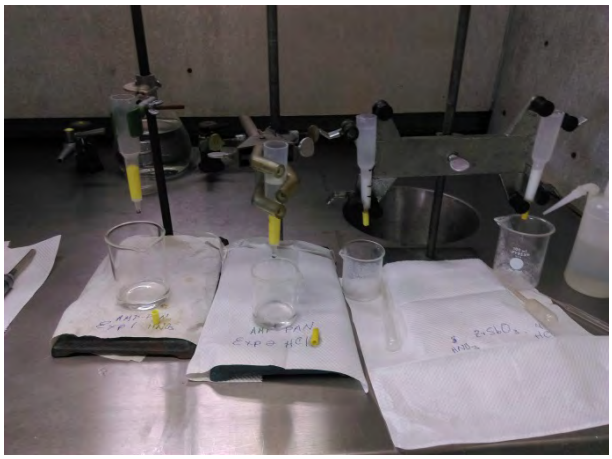

Figure 2. AMP-PAN filtration columns to trap ^{137}Cs from acid solution and exchange it into a basic solution.

Figure 3. Activity detection of ^{137}Cs-^{137m}Ba standard acid solution before filtration, and after recovery of radioactive pair in basic solution.

$\lambda_2\left({}^{137m}\mathrm{Ba}\right) = 0.693/2.55 = 0.272\,\mathrm{min}^{-1}$. Therefore, the difference between the larger one λ_2(^{137m}Ba) and the smaller one λ_1(^{137}Cs) is negligible: 0.272 − 4.385 × 10^{-8} = 0.27199, while the quotient between the larger and the smaller one is very great: 0.272/4.385 × 10^{-8} = 6.203 × 10^6. So, when this radioactive pair is separated, their radioactive equilibrium ($A_1 = A_2$, $\lambda_1 N_1 = \lambda_2 N_2$, where $\lambda_2 \gg \lambda_1$ and $N_1 \gg N_2$), is recovered in only 3.68 minutes. In this way, if the equation proposed by G. R. Choppin [6], to evaluate either number of daughter or parent nucleus in radioactive equilibrium, as a function of λ_1 and λ_2, when half lives of both are in a relation from days to hours (not so great as years to minutes), may be simplified, since the difference $\lambda_2 - \lambda_1$ is negligible (0.272 − 4.385 × 10^{-8} = 0.27199), and we can consider that:

$$N_2 = \lambda_1 N_1/\left(\lambda_2 - \lambda_1\right) \text{ is the same that } N_2 = \lambda_1 N_1/\lambda_2 \text{ and } N_1 = N_2\lambda_2/\lambda_1$$

As a matter of fact, it is possible to use for this case the simpler equation of radioactive father and daughter in equilibrium: $A_1 = A_2$, $N_1\lambda_1 = N_2\lambda_2$, $N_1 = N_2\lambda_2/\lambda_1$, where $\lambda_2/\lambda_1 = K$ (constant value). It means that constant value K is equal to quotient $t_{1/2(1)}/t_{1/2(2)} = 0.272/4.358\times10^{-8} = 6.241\times10^6$.

So, if a number of nucleus are counted by mass number, for the isobaric pair ^{137}Cs-^{137m}Ba, will be obtained some number R, sum of $N_1 + N_2 = R$, where N_2 may be replaced by its value $N_2 = \lambda_1 N_1/\lambda_2$, and in such a case $N_1 + \lambda_1 N_1/\lambda_2 = R$, and $N_1\left(1+\lambda_1/\lambda_2\right) = R$. But if it is considered that 1 + 6.241 × 10^6 is equal to 6.241 × 10^6 for our purpose, then N_1 = R/6.241 × 10^6, which means number of ^{137}Cs atoms, while $R - N_1 = N_2$, ^{137m}Ba number of daughter atoms in all cases. Therefore, if it is related the atoms number of radioactive contaminant ^{137}Cs, with atoms number of natural radioactive ^{40}K, in order to evaluate the intensity of radioactive contamination in marine sediments, we have to consider that in the extremely remote case the activity of contaminant ^{137}Cs could reach up that of natural ^{40}K, the meaning of that unlikely but possible event, should be 2.35 single atoms of ^{137}Cs related to 1 × 10^8 atoms of natural ^{40}K, because: $t_{1/2}\left({}^{137}\mathrm{Cs}\right) \ll t_{1/2}\left({}^{40}\mathrm{K}\right)$ and $\lambda_1\left({}^{137}\mathrm{Cs}\right) \gg \lambda_2\left({}^{40}\mathrm{K}\right)$. Consequently, if $A_1\left({}^{137}\mathrm{Cs}\right) = A_2\left({}^{40}\mathrm{K}\right)$, then $N_1\lambda_1\left({}^{137}\mathrm{Cs}\right) = N_2\lambda_2\left({}^{40}\mathrm{K}\right)$ and

$$N_1\left({}^{137}\mathrm{Cs}\right)/N_2\left({}^{40}\mathrm{K}\right) = \lambda_2\left({}^{40}\mathrm{K}\right)/\lambda_1\left({}^{137}\mathrm{Cs}\right) = t_{1/2}\left({}^{137}\mathrm{Cs}\right)/t_{1/2}\left({}^{40}\mathrm{K}\right)$$
$$= 30.07 \text{ years}/1.28\times10^9 \text{ years} = 2.35\times10^{-8} = 2.35/10^8 .$$

Time calculation to get the radioactive equilibrium between parent ^{137}Cs (valence 1), and daughter ^{137m}Ba (valence 2), after their separation by using ion exchange resins.

After recovery with a very basic solution (pH = 9.5) the ^{137}Cs ($t_{1/2}$ = 30.17 years), from the exchange resin, it is estimated the necessary time to get up the radioactive equilibrium with her daughter ^{137m}Ba ($t_{1/2}$ = 2.55 m). So, if it is named N_1 the number of parent atoms and N_2 the number of daughter atoms, λ_1 and λ_2 decay constants for parent and daughter respectively, at time zero the sample has only N_1 and no N_2, but the time starts and N_2 begins to grow up, according the next equation:

$$N_2 = \left(N_1 - N_1 e^{-\lambda_1 t}\right) e^{-\lambda_2 t} = N_1 e^{-\lambda_2 t} - N_1 e^{-(\lambda_1+\lambda_2)t} = N_1\left(e^{-\lambda_2 t} - e^{-(\lambda_1+\lambda_2)t}\right)$$

where the time function $f(t) = e^{-\lambda_2 t} - e^{-(\lambda_1+\lambda_2)t}$ determines the daughter ^{137m}Be growing up by the parent ^{137}Cs decaying, and the first derivative $f'(t)$ equal 0 means the time when N_2 stops growing and gets the equilibrium with parent, that is to say $N_1\lambda_1 = N_2\lambda_2$ and radioactive equilibrium $A_1 = A_2$:

$$f'(t) = -\lambda_2 e^{-\lambda_2 t} + (\lambda_1+\lambda_2) e^{-(\lambda_1+\lambda_2)t} = 0$$

$$\lambda_2 e^{-\lambda_2 t} = (\lambda_1+\lambda_2) e^{-(\lambda_1+\lambda_2)t}$$

$$\lambda_2 / (\lambda_1+\lambda_2) = e^{-(\lambda_1+\lambda_2)t} / e^{-\lambda_2 t} = e^{-\lambda_1 t} = 1/e^{\lambda_1 t}$$

$$e^{\lambda_1 t} = (\lambda_1+\lambda_2)/\lambda_2 = \lambda_1/\lambda_2 + 1$$

$$\lambda_1 t = \ln(\lambda_1/\lambda_2 + 1)$$

$$t = \ln(\lambda_1/\lambda_2 + 1)/\lambda_1$$

Therefore:

$$\lambda_1 = 0.693/30.17 \times 365 \times 24 \times 60 = 4.37 \times 10^{-8}\ \text{min}^{-1}$$

$$\lambda_2 = 0.693/2.55 = 0.272\ \text{min}^{-1}$$

$$t = \ln\left(1 + 4.37 \times 10^{-8}/0.272\right)/4.37 \times 10^{-8} = 3.68\ \text{min}$$

3. Results

Due to great difference between both radioisotopes: contaminant (^{137}Cs, $t_{1/2}$ = 30.17 years) and natural (^{40}K, $t_{1/2}$ = 1.28 × 10^9 years), their decay constants are much greater for the minor half life (^{137}Cs, $\lambda_1 = 0.693/30.17 = 2.297 \times 10^{-2}$ years^{-1}) than that of much greater half life (^{40}K, $\lambda_2 = 0.693/1.28 \times 10^9 = 5.414 \times 10^{-10}$ years^{-1}). Therefore, for a given number of nucleus, the radioactivity of contaminant ^{137}Cs should be much greater than that of natural ^{40}K for a factor equal to 4.243 × 10^7 times. But fortunately, this has not been the case for any sample examined till now, where the RCF has not surpassed 11.4% [7]. But this light contamination also implies the continue production of ^{137m}Ba($t_{1/2}$ = 2.55 m), γ rays emitter, which decays by isomeric transition to ^{237}Ba, in mass not appreciable to surpass the natural percentage (11.23%) of this isotope in natural elementary Ba found in marine sediment samples, which could happens with much more appreciable contamination by radioactive ^{137}Cs. So, to get the contamination by ^{137}Cs in terms of mass percentage related to one gram of marine sediments, once separated natural Ba and ^{137m}Ba from contaminant ^{137}Cs by capture the ^{137}Cs from the cation exchanger, after 3.68 minutes radioactivity from parent ^{137}CS and daughter ^{137m}Ba get the radioactive equilibrium in which A_1(^{137}Cs) = A_2(^{137m}Ba). But $N_1\lambda_1$ = $N_2\lambda_2$ implies that N_1(^{137}Cs) = $\lambda_2 N_2$(^{137m}Ba)/λ_1, and ICP-MS gives us the counts per second obtained only from ^{137m}Ba nucleus previously separated of natural ^{137}Ba, and so ^{137}Cs = ^{137m}Ba × $t_{1/2}$(^{137}Cs)/$t_{1/2}$(^{137m}Ba), both half lives expressed in minutes. Therefore, when number of ^{137}Cs atoms is compared with Avogadro's number (6.02 × 10^{23} atoms) for the molecular weight of it (137 g), we

Table 1. Mass of contaminant ^{137}Cs in Cuban marine sediments, obtained by mass spectrometry.

Sample From	Sample Weight (grams).	^{137m}Ba count/sec. (mass. spect.)	^{137}Cs Atoms number	^{39}K c/sec. (mas.spect.)	^{40}K Atoms number	pg^{137}Cs/g. sample
Nautico	1.0644	5.98×10^{4}	3.7×10^{11}	7.03×10^{7}	8.92×10^{3}	79.
Guanabo	1.0103	2.90×10^{4}	1.8×10^{11}	7.63×10^{7}	9.68×10^{3}	41
Bibijagua	1.0227	4.17×10^{4}	2.6×10^{11}	1.36×10^{8}	1.72×10^{4}	58
Batabano	1.0168	3.10×10^{4}	1.92×10^{11}	5.75×10^{7}	7.30×10^{3}	43

obtain the weight of contaminant ^{137}Cs present in determined mass of sediment sample, per gram when divided by the weight sample. Even when elementary K is separated in the exchanger resin together with ^{137}Cs-^{137m}Ba, and also present in the basic final solution with radioisotope ^{40}K, it is not possible to obtain the number of ^{40}K atoms by ICP-MS, because gaseous ^{40}Ar mass is used to form the necessary plasma where bivalent cations ^{137m}Ba are counted by second. Nevertheless, it is quite possible to count ^{39}K atoms, which have one constant proportion in elementary K equal to 93.22%, and comparing this figure with that of ^{40}K (0.0118%), it is obtained the number of ^{40}K atoms present in the weight of marine sediments treated, and responsible of the natural radioactivity in the marine sediment sample. So, Table 1 shows the results obtained in four samples of Cuban marine sediments, previously detected for ^{137}Cs radioactive contamination, in order to compare it with natural ^{40}K radioactivity [7], and at present using mass spectrometry instead disintegrations by time units.

4. Conclusion

Even when cation exchanger AMP-PAN results highly efficient to separate ^{137}Cs from the marine sediments, and it shows to separate also elementary K, since the characteristic 1.46 Mev peak of ^{40}K appears in the final basic solution filtered by the resin, the number of ^{39}K detected by mass spectrometry as counts per second appears to be lower than that obtained by ^{40}K radioactive detection at known efficiency, comparing 0.0118% as isotope abundance of ^{40}K with 93% of ^{39}K. It seems to demonstrate that only a fraction of K much more abundant that contaminant Cs present in the sediment, appears in the final basic solution filtered in the resin. On the other hand, ^{137}Cs-^{137m}Ba mass separation results 97% - 99% efficient, and it allows to calculate directly the mass of contaminant ^{137}Cs in atoms number as well as ^{137}Cs (10^{-12} g) (picograms) per gram of sample.

Conflicts of Interest

The authors declare no conflicts of interest regarding the publication of this paper.

References

[1] Becker, J.S. (2005) Recent Developments in Isotope Analysis by Advanced Mass

Spectrometry Techniques. *Journal of Analytical Atomic Spectrometry*, **20**, 1173-1184. https://doi.org/10.1039/b508895j

[2] Navarrete, J.M. and Müller, G. (2010) Natural Radioactivity and Radioactive Contamination in Sea Water. *Radioactive Contamination Research Developments*, Nova Science Pub, **8**, 270-274.

[3] Navarrete, J.M., Espinosa, G., Müller, G., Golzarri, J.I., Zúñiga, M.A. and Camacho, M. (2013) Marine Sediments as a Radioactive Pollution Repository in the World. *Journal of Radioanalytical and Nuclear Chemistry*, **299**, 843-847. https://doi.org/10.1007/s10967-013-2707-4

[4] Roy, K., Pal, D.K., Basu, S., Nayak, D. and Lahiri, S. (2002) Synthesis of a New Exchanger, Zirconium Vanadate, and Its Application to the Separation of Barium and Cesium Radionuclides at Tracer Levels. *Applied Radiation and Isotopes*, **57**, 471-474. https://doi.org/10.1016/S0969-8043(02)00136-7

[5] El-Khouli, S.H., Attalah, M.F. and Allan, K.F. (2013) Studies on Separation of Cs/Ba and Zn/Cu Binary Mixtures on Zirconium Antimonate as Ion Exchanger. *Russian in Radiokhimiya*, **55/5**, 407-412. https://doi.org/10.1134/S1066362213050068

[6] Choppin, G.R. and Rydberg, J. (1980) Nuclear Chemistry, Theory and Applications. Pergamon Press, 70.

[7] García Batlle, M. and Navarrete, M. (2018) Marine Sediments as Fundamental Repository of Radioactive Contaminants in Aquatic Ecosystems. *Sedimentation Engineering*, IntechOpen, 173-186. https://doi.org/10.5772/intechopen.72053

World Journal of Nuclear Science and Technology, 2020, 10, 39-46
https://www.scirp.org/journal/wjnst
ISSN Online: 2161-6809
ISSN Print: 2161-6795

Analysis of Materials for Heat Transport in Tokamaks

Márcio Belloni, Thadeu das Neves Conti

Institute of Energy and Nuclear Research, São Paulo, Brazil
Email: prof.belloni@gmail.com, tnconti@gmail.com

How to cite this paper: Belloni, M. and das Neves Conti, T. (2020) Analysis of Materials for Heat Transport in Tokamaks. *World Journal of Nuclear Science and Technology*, **10**, 39-46.
https://doi.org/10.4236/wjnst.2020.101005

Received: September 24, 2019
Accepted: December 16, 2019
Published: December 19, 2019

Copyright © 2020 by author(s) and Scientific Research Publishing Inc.
This work is licensed under the Creative Commons Attribution International License (CC BY 4.0).
http://creativecommons.org/licenses/by/4.0/
Open Access

Abstract

Every nuclear power reactor, whether of fusion or fission, is essentially a thermal system that generates electricity. In this sense, there are several problems in relation to this heat transport. The model of plasma confinement by magnetic force, in the nuclear fusion (sterellator and tokamak), has only been 20 years and recently some success in the quality of the generated plasma has been achieved. However, due to the large amount of energy coming from the plasma, the choice of the material that will carry the generated energy is quite troublesome, due to the need to handle a very high temperature for the nuclear fission standards. Solutions are explored by the scientific community to transport the energy generated in the case of the primary circuit, after exceeding breakeven temperature and models that are based on the fission reactors of the fourth generation and those currently in operation, to search for solutions regarding the transport of heat generated for the generation of electric energy. Several materials such as pressurized water, sodium, helium and boron have been considered and studied to form the primary heat transfer circuit for the exchanger. A thorough analysis of these materials is necessary. This research looked at some of these materials for heat transport and power generation. Lithium and helium were found to be the probable materials for conveying heat and cooling in the blanket. The results show that research on blanket materials needs more attention. The quality of these materials needs to be improved by material research, with the ODS EUROFER alloy and other research to reduce material erosion by helium nano bubbles. Plasma quality needs to be improved to keep constant and free of impurities when using lithium in liquid form.

Keywords

Thermonuclear Fusion, Tokamak, Renewable Energy, ITER Project, Material Analysis

1. Introduction

In any system of electric power generation based on thermodynamics, it is used the transfer of thermal energy for its transformation into mechanical energy, basically to move turbines generating electric energy. Thus, in a hypothetical reactor of nuclear fusion, there is great difficulty in taking advantage of the heat generated.

2. Objectives

This study aims to analyze the best means of transport of the energy produced in tokamak type nuclear fusion reactor for the generation of renewable electric energy.

3. Methodology

The hypothetical-deductive method is presented. Bibliographic research was conducted to collect knowledge about controlled thermonuclear fusion and tokamak operation, as well as fourth generation reactors and those currently in operation. Visits were also made to the USP Institute of Physics (IFUSP) plasma studies laboratory to learn about the on-site tokamak and visits to the Energy and Nuclear Research Institute (IPEN/CNEN) to learn about the current model of nuclear fission and the perspectives on nuclear fusion. At these sites, questions were asked about the experimental tokamak and the IEA-R1 nuclear reactor to learn how core and plasma heat are mobilized.

4. Development

It is recognized that the basis of any study on tokamak nuclear fusion is supported by three fundamental pillars, namely, the study of the nuclear forces involved, the study of electromagnetism used for magnetic plasma containment, particle thermodynamics, hydrodynamics of the plasma [1].

The plasma state required for nuclear fusion, is by its nature an ionized gas. In this sense, the protons are free of their electrons so they have a very considerable repulsion force, forming a barrier of repulsion, and must be approximated enough that the hadronic force, offered by the gluons, renders hydrogen isotopes in a new element, that is, helium. To overcome this barrier, heat is supplied to the plasma by increasing the kinetic energy of the particles by changing the atomic mass of the isotopes. This is done by delivering thermal energy to the plasma [2].

The amount of heat generated poses a great challenge in the transportation of this heat, and at this moment it is necessary to pay attention to the related phenomena. Due to the fact that the plasma is vacuum-packed, the use of the generated heat avoids the convection caused by air, which would also disturb the integral of the plasma. On the other hand, this also decreases the value of the energy used, since with the vacuum, only the thermal radiation and the emission of neutrons can be considered. The conduction of heat does not occur because

the conductive element is missing. But even with only elements of thermal radiation and fast neutrons, it is necessary to study in detail the element that is sufficiently resistant to the point of effecting the exchange of thermal energy with the plasma.

In the tokamaks, a structure is used that serves as moderator element and also captures the heat generated. This is the "blanket", which is created with material that absorbs the fast neutrons by performing several important roles in the fusion reactor. First, it reduces the speed of the neutrons and particles emitted in the fusion and also attenuates the generated heat, in order to protect the exterior of the reactor, also, avoiding that the plasma interferes in the generation of the created electromagnetic field, that must be in low temperature. In the case of ITER, electromagnets made from superconductors require temperatures in the order of −269˚C [3].

In the ITER project, as in **Figure 1**, the blanket system coats the inner surface of the vacuum chamber, and its main function is to provide shielding for the chamber and the superconducting magnets of the heat flux and the neutron flux, as the neutrons passing through this system are moderate, the kinetic energy of the neutrons is transformed into heat is transferred to the refrigerant for the purpose of generating electricity. The ITER blanket system is one of the most problematic along with the diverse system due to the fact that they will be the first contact of the radiation emitted by the hot plasma. Currently the material to be used in this system is beryllium due to its physical properties and possibly at a later stage a tritium regenerative blanket system will be tested [4].

In this way, one must choose the most suitable material for such capture of the thermal radiation. If on the one hand the material must be a good conductor of heat, it must also be sufficiently resistant to the radiation of the X-rays, high-speed neutrons and α particles emitted in the fusion, thus avoiding to change the structure of the material [4].

It is possible to have an idea of the value of heat if you consider the system as ideal according to the theory of the blackbody and the monochromatic emissive

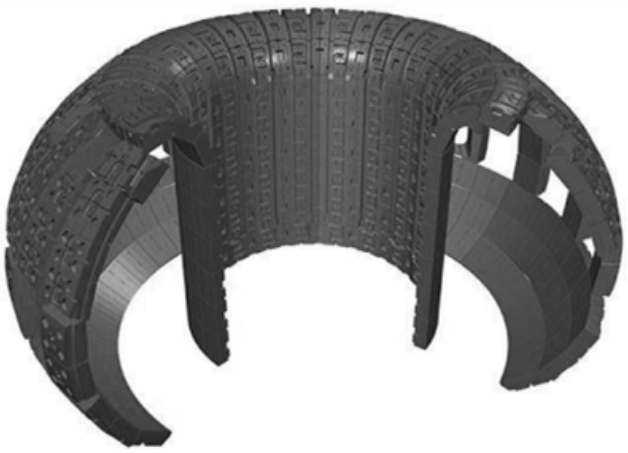

Figure 1. Blanket of the ITER tokamak. Source: CABRERA (2013).

power. It is obtained by integrating the monochromatic emissive power over the entire wavelength range [5]. In this sense, the value of integration results in the mathematical model:

$$E_n = \sigma \cdot T^4 \tag{1}$$

If the system behaves as a blackbody in which there is a state of equilibrium between particles and the radiation field, the flux of radiation from the surface is expressed by Stephan-Boltzmann's law [6].

$$I = \propto \cdot T^4 \tag{2}$$

Analyzing the mathematical model proposed by Boltzman, one can reach the temperature value to overcome the repulsion barrier. One of the most latent problems of the fusion reaction is precisely its greatest advantage: the heat. A nuclear fusion reactor generates more than 10^9 K.

Materials Used

The temperature, in the tokamak, is captured by the "blanket" that has the condition of protecting the exterior systems of the containment vase. In the "blanket", channels where the refrigerant circulates, transport the generated heat to the secondary circuit, besides cooling the structure so that the emission of heat and radiation does not occur in the form of α particles, high speed neutrons and x-rays for the external tokamak systems, such as electromagnets. This time, the material from which the "blanket" is made must be a little reactive and capable of decelerating neutrons, where beryllium, graphite or tungsten are recommended.

In the example of ITER, in **Figure 2**, the blanket covering a surface of 600 m^2 is one of the most critical and technically challenging components. Along with the diverter, it directly faces the hot plasma.

Due to its unique physical properties (low plasma contamination, low retention

Figure 2. Blanket of the ITER. Source: ITER Organization. ITER Project web site.

of fuel), beryllium was chosen as the element to cover the first wall in that case. The rest of the blanket modules will be made of copper and high strength stainless steel (EUROFER). ITER will be the first fusion device to operate with an actively cooled blanket, the cooling water will be injected at 4 MPa and 70˚C and will remove up to 736 MW of thermal energy.

Although ITER will use water, which is pressurized, it can transport more energy without reaching the critical state [3]. But for a reactor with the power to generate electricity commercially and effectively, it is not the best option, even possessing the versatility of being abundant, cheap and easy to control. Its low boiling point avoids its use in high efficiency reactors.

Like the fast generation 4th generation reactors, sodium, which is already studied in several reactor projects of this generation, is a very interesting alternative. In this understanding, Wilma dos Santos Bastos explains that the use of sodium is a mature and dominated technology. Its use in the exchanger is very feasible, since it is already known the use of sodium in reactors of Japanese 4th generation with power of 1500 MW (JSFR). One of its greatest advantages are:

1) high thermal conductivity (68.8 W/m·K at 450˚C);

2) high temperature (≈550˚C);

3) Corrosion caused by sodium is easily controlled [7].

In the same comparative sense, it is possible to analyze the nuclear reactors of the type HTGR that can reach, in the refrigerant fluid, the temperature of 750˚C to 1000˚C. In these reactors, a lot of the helium is used, because the same one is inert chemically, has a low neutron absorption shock section and has good properties with respect to heat transfer. The use of conventional coating materials, such as stainless steel, is not necessary [8].

However, many authors point to Lithium as the best option for transporting the generated energy. (US Nuclear Energy Policy Study Group, 1971, page 194). More precisely, its Li^7 isotope [9]. This is justified because the melting and boiling point of lithium is higher than the other elements of group I, being of 181˚C and Boiling is of 1347˚C. The bombardment of Lithium Isotope will generate Tritium (H^3). This explains the authors' preference. The atomic interactions between the ^{7}Li isotope and the fast neutrons produced by nuclear fusion make Lithium the best option for heat transport. In addition, the increase in pressure in the primary circuit may raise the boiling point of the lithium, causing it to carry a much larger amount of heat. The reaction with the lithium will generate the tritium that can be used by the own reactor since it will suffer the shock with fast neutrons. In the reactor, it will be produced locally by neutron bombardment (produced in the fusion reaction) of the fertile lithium layer [10]. Thus, they have the following reaction.

$$^{0}\mathrm{Li} + {}^{1}\mathrm{n} \rightarrow {}^{4}\mathrm{He} + {}^{3}\mathrm{H} \quad [11] \tag{3}$$

The model of regeneration of lithium and removal of the tritium generated, to serve as fuel in the plasma. Recovery of the tritium would be done by cooling the lithium to a temperature near its melting point, filtering the precipitated Li/T

and heating it to its decomposition temperature by a distillation or gas extraction process. However, problems to pump lithium by an extreme electromagnetic field are circumvented by several hypotheses but without a conclusion.

Several methods have been discussed to solve the problem of the great power needed to pump the lithium into a strong magnetic field. There is a possibility to coat the lithium-containing tubes with a nonconductive material, but pumps that move the fluidic lithium should pay special attention. Research shows that DC electromagnetic pumps have yielded great results in this case. These pumps have no moving parts and need no further maintenance.

Spitzer also mentions this possibility and suggests that such material should not be corrosive or brittle. The fact that the insulation material has to withstand corrosion by hot lithium and thermal stresses involves serious technical problems. He also studied the possibility of lithium remaining stagnant and the removal of blanket heat with water [12].

A model of nuclear fusion reactor, in **Figure 3**, demonstrates how to capture the heat generated. In this case, it is verified that the transport is effected by radiation, since the plasma makes impossible the conduction or convection [10].

In the case of fusion reactors, helium is the product of the reaction and can be collected and used in the cooling and energy transport system. The use of helium is supported by several researchers, including the fact that the projected commercial tokamak models use new material for their structure, ferrostic-martensitic hardened by dispersion of oxides and denominated (ODS EUROFER) for structural use. Thus, helium is indicated by its reaction with this alloy. It occurs that the helium has low susceptibility with respect to the ODS EUROFER alloy [13].

Big problem encountered is the corrosion caused by helium when in contact with metals. According to tests, helium, when in contact with metals, in nuclear reactions, form bubbles of nanometric size. These bubbles, when in large numbers, collide forming larger bubbles (in order of micrometer), causing the destruction

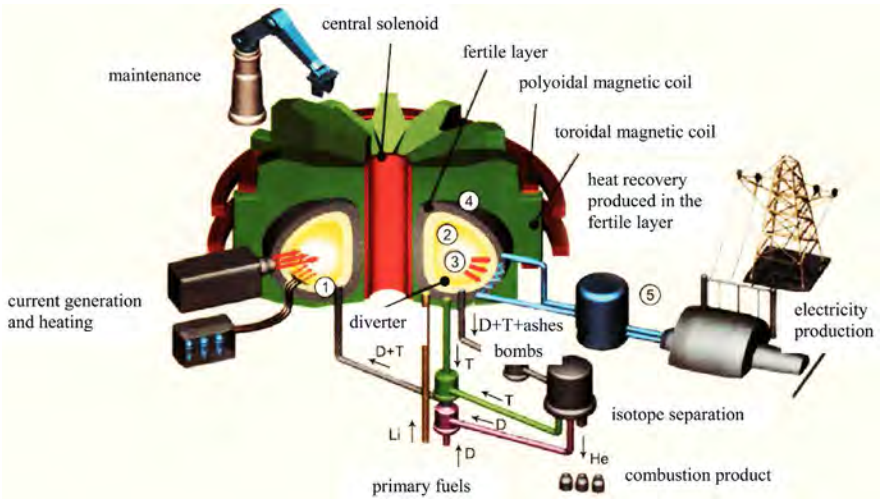

Figure 3. Nuclear fusion reactor model and the lithium blanket. Source: Manso and Varandas, 2009, p. 71.

of the material. It has been found that multilayer copper and niobium composites have caused capillaries formed by deposited helium and not bubbles.

These capillaries will act as channels through which helium can escape, without damaging the structure. Thus, structural integrity will be maintained, and there will be a slight leakage of the helium contained in the material, *a priori*.

5. Conclusions

Tokamak is observed to be the most likely reactor for generating electricity efficiently. Especially with the ITER project, controlled thermonuclear fusion for power generation is getting closer and closer to reality. There is also a possibility to use various generated coolants and heat absorbers, including pressurized water, lithium, helium and sodium.

This time, we should look at existing technology, both in what is already used in the operation of reactors such as Angra 1 and 2, as well as the fact that it has a lot of risk and accident documentation, as in new projects like advanced nuclear reactors. Fourth generation reactors provide much of the material already questioned in the new nuclear refrigerants, although it was never a reactor that supplied as much energy as a large fusion reactor like the ITER project. To proximity to the hot plasma the better material is the lithium in liquid state and the helium because the actual material studs and the physicochemical features. Lithium is an option for heat transport because its physicochemical features are very interesting for the system. In the liquid state, it is easier to contain lithium in the primary circuit and changer, but lithium cooling should be avoided to prevent fluid loss (LOCA) even in case of plasma cooling. Very easily, according to the tests observed in the existing experimental tokamaks. Thus, with regard to lithium, studies on plasma maintenance are required to be constant and homogeneous, respecting Lawson's law.

In addition, as it is already used in fission reactor designs and is the product of hydrogen fusion of nuclear isotopes, helium is seen as an elegant and effective solution for transporting the heat generated in nuclear fusion. The corrosion problem observed in the literature, where helium lodges in metals such as nano-filled bubbles, causing its destruction, is being addressed in studies of innovative alloys such as ODS EUROFER and techniques for the use of niobium and multilayer copper metals. Helium circulation channels facilitate even the separation of other gases. The choice is then to use helium and lithium for their physicochemical characteristics and the research so far pointed out.

Conflicts of Interest

The authors declare no conflicts of interest regarding the publication of this paper.

References

[1] Belloni, M. (2017) Sub-Atomic Particles for Effectiveness in Controlled Thermonuclear Fusion Reactions. *Proceedings of the* 24*th International Symposium on*

Scientific and Technological Initiation of USP, Sao Paulo.

[2] Belloni, M. (2017) The Thermonuclear Fusion Process the Thermonuclear Fusion Process. *Proceedings of the Week of Science and Technology*, Guarulhos.

[3] ITER Organization. The International ITER Project for Fusion: Why? Website of the ITER Project. Electronic Document. https://www.iter.org

[4] Cabrera, C.E.V. (2013) Neutron Evaluation of the Insertion of a Transmuting Layer into a Tokamak System. Dissertation (Master's Degree), UFMG, Minas Gerais.

[5] Schimidt, F.W., Hendereson, R.E. and Wolgemuth, C.H. (1996) Introduction to Thermal Sciences: Thermodynamics, Fluid Mechanics and Heat Transfer. Ed Blucher, São Paulo.

[6] Tomimura, A. (1980) Controlled Thermonuclear Fusion. Nuclear Energy. Military Engineering Institute, Ministry of the Army, Rio de Janeiro.

[7] Bastos, W.S. An Introduction to IV Generation Rapid Reactors. http://www.ipen.br

[8] Terremoto, L.A.A. (2004) Fundamentals of Nuclear Reactors Technology. http://www.social.stoa.usp.br

[9] Ribeiro, G.F. Diagnosisoflithium; Braziliansituation. CNEN, Rio de Janeiro. http://www.iaea.org

[10] Manso, M.E. and Varandas, C.A.F. (2009) Nuclear Fusion, an Energetic Option for the Future. Physics Gazette, Vol. 29, Lisbon.

[11] Coelho, P. (2013) Hydrogen Isotopes: Deuterium and Tritium. http://www.engquimicasantossp.com.br

[12] Carvalho, S.H. (1980) Blanket for Fusion Reactors: Materials and Neutron. Master Degree Dissertation, Federal University of Rio de Janeiro, Rio de Janeiro.

[13] Zimmermann, A.J.O., Sandim, H.R.Z. and Padilha, A.F. (2010) The New EUROFER Stainless Steels Used in Nuclear Fusion. *Rem Revista Escola de Minas*, **63**, 287-292. https://doi.org/10.1590/S0370-44672010000200012

World Journal of Nuclear Science and Technology, 2020, 10, 47-64
https://www.scirp.org/journal/wjnst
ISSN Online: 2161-6809
ISSN Print: 2161-6795

Feasibility of "Rooppur Nuclear Power Plant" & Its Contribution to the Future Energy Sector

Antu Biswas[1], Md. Shivly Mahmood[2]

[1]Department of Automation, National Research Nuclear University MEPhI, Moscow, Russia
[2]Department of Nuclear Science and Technology, Harbin Engineering University, Harbin, China
Email: antubiswas188@yahoo.com

How to cite this paper: Biswas, A. and Mahmood, Md.S. (2020) Feasibility of "Rooppur Nuclear Power Plant" & Its Contribution to the Future Energy Sector. *World Journal of Nuclear Science and Technology*, **10**, 47-64.
https://doi.org/10.4236/wjnst.2020.101006

Received: November 18, 2019
Accepted: December 21, 2019
Published: December 24, 2019

Copyright © 2020 by author(s) and Scientific Research Publishing Inc.
This work is licensed under the Creative Commons Attribution International License (CC BY 4.0).
http://creativecommons.org/licenses/by/4.0/
Open Access

Abstract

Digital Bangladesh is one of the most challenging decisions made by the government to transform the country to be a middle-income country by 2021. That's why the government implemented a large number of projects relating to digital technology. Rooppur Nuclear Power Plant (RNPP) project is one of them. In the recent past, the country faced an enormous electricity shortage with a great energy gap between peak demand and maximum energy generation. In Bangladesh, the present government promised to ensure the electricity to all the citizens by 2021. That's why the world's most lucrative Nuclear advanced technology is going on under Power Sector Master Plan (PSMP)-2016 (Vision 2041). In order to improve the security system of nuclear power, the bilateral project is not fully transparent for the public, which is understandable. That makes some political conflict with the anti-nuclear agenda. As a result, the general concerns are also involving in this project. Safety and Security systems by the world's most advanced Water-Water Energy Reactor (VVER-1200) is in full discussion by this paper in order to get rid of local concerns. Countries Power Profile is completely described and focuses on the current National Planning to overcome the power shortage through the use of Nuclear Power. This paper mainly discusses the feasibility of RNPP in Bangladesh and how it will play a major role in the national energy sector in future to become the "DREAM COME TRUE" project for Bangladesh.

Keywords

Digital Technology, RNPP, Energy Gap, PSMP, Feasibility

1. Introduction

In the recent past, Bangladesh is struggling very much in order to meet the energy demand. Day by day the situation got crazier. The huge population and

their upcoming demand for technological advancement made it very much tough for the power generating sectors to fill up the gap between energy demand and energy generation. As a result, the Government of Bangladesh took some responsible plans matched with some huge technological advancement like "Rooppur Nuclear Power Plant" project [1]. Rooppur Nuclear Power Project is one of the dream projects for Bangladesh. With the help of this project, Bangladesh will be the 33rd country has nuclear power profile. That can contribute 2400 MW power in the grid system to meet up the energy demand. The complex nuclear technology that has run under the financial and technological support of ROSATOM.

2. Energy Information

2.1. Structure of Electric Power Sector

In Bangladesh, Ministry of Power, Energy & Mineral Resource (MoPEMR) manages the electricity business. Where the power is generated by Bangladesh Power Development Board (BPDB), power plants that are departments and subsidiaries of BPDB, Independent Power Producer (IPP), and private power generation companies. Power is supplied through Power Grid Company of Bangladesh's (PGCB) power transmission facilities to customers in local cities by BPDB, in the metropolitan area by Dhaka Power Distribution Company Ltd. (DPDC) and Dhaka Electric Supply Distribution Company (DESCO), and in rural areas by Palli Biddyut Samities (PBS). And the distribution departments in local cities are being separated one by one [2].

2.2. Contribution of Different Power Generation Sectors

2.2.1. Energy Scenario

The conventional technique is applied by Bangladesh, as a reason energy is less sufficient and unorganized. Where Bangladesh has one of the least per capita utilization of about 332 KWh in the world [3]. Where Bangladesh has nearly 2000 mt reserves of coal and around 14.15 tcf amount of natural gas reserves. Which is not in the huge amount [4]. Natural gas, oil, hydropower, and coal are the commercial source of energy utilization. **Figure 1** shows the power generation scenario of Bangladesh [5].

2.2.2. Contributions of Public & Private Sector

In the current situation, both public and private power generation is equally important. Here is an overview by **Figure 2**. In Bangladesh private sectors provides almost 50% of the total power generation. Among the public sectors BPDP alone provides almost 4402 MW and privates sectors IPPs provides 3245 MW. It is clear that the public sector does not generate sufficient load to meet the public demand. 3/5 years Rental plants are providing about 55% load from private sector generation which is very costly. Those cost 20 tk/Unit, which is a very high amount [5].

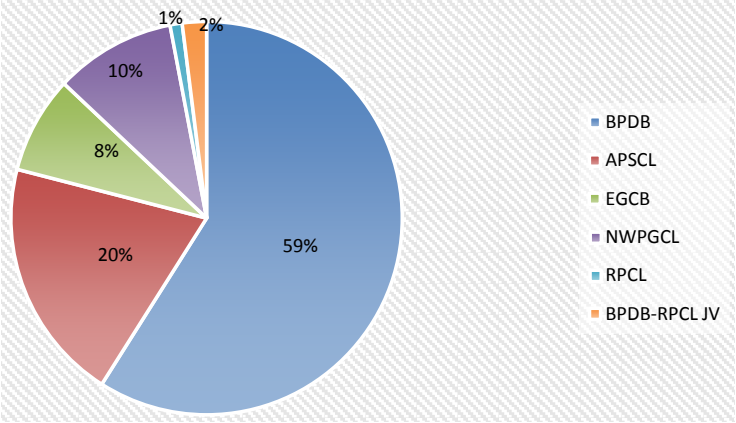

Figure 1. Energy scenario of Bangladesh.

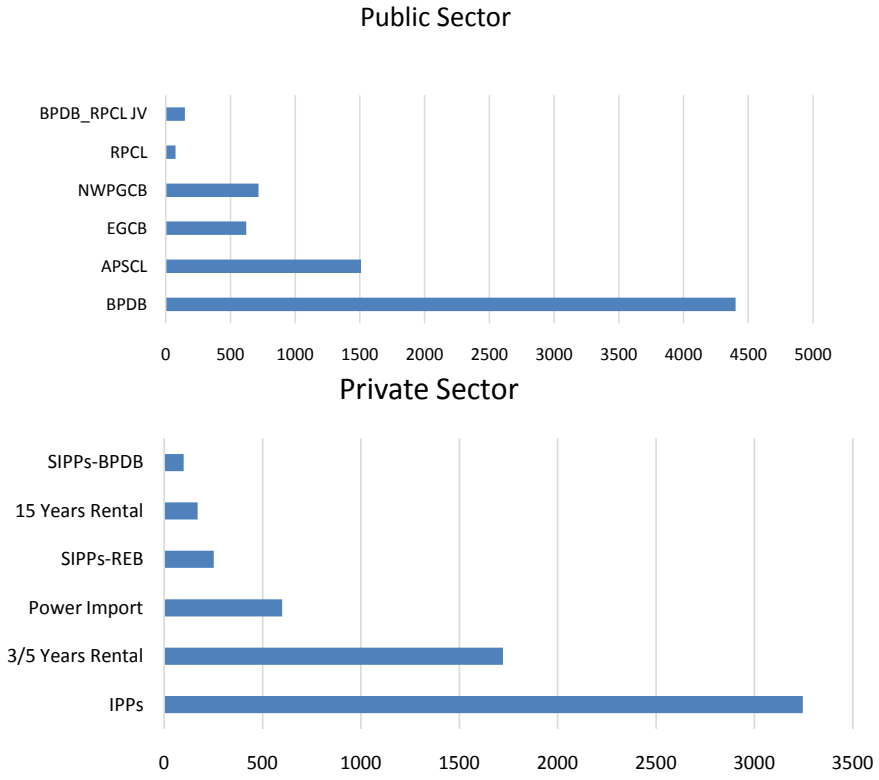

Figure 2. Public & private sector contribution in national grid.

2.3. Power Stations in Bangladesh

Bangladesh is so much dependent on its tradition energy technology leading by the natural gas (62.39%). Although furnace oil (20.49%), diesel (7.97%), coal (2.33%), hydro (2.15%) makes a vital role in energy generation [6]. Until the mid-1990s demand for fertilizer was the top priority. But, now a day's demand for the gas power generation has risen. The fastest-growing demand is from the industry, with 13% annual increase [7] shown in the **Table 1**. Power contributions and the National energy statistics are also described briefly by the **Table 2** and **Table 3** correspondingly.

Table 1. Demand of natural gas, 1991-2007.

Sector	Average annual growth rate
Power	8.2%
Fertilizer	3.9%
Industry	12.6%
Domestic	12.0%
total	7.7%

Table 2. Power station summary.

Fuel Type	Running Power Plants			Plant Under Construction			
	Power Stations	Capacity (MW)	Ref.	Power Stations	Capacity (MW)	Expected Operations	Ref.
Coal Fired	Barapukuria	525	[8]	Matarbari	1200	2024 [8]	[9]
				Payra Thermal	1320	1st unit in August, 2019 [10]	[11]
				Rampal	1320		[11]
Oil & Gas Fired	Ashuganj	1627	[12] [13]	Feni Lanka Power Limited	114	September, 2019	
	Ghorasal	950	[14]				
	Shikalbaha	150		Manikganj Power Generations Limited	162	January, 2020	
	Siddhirganj	260					
	Orion Group	4*100		Bhairob Power Limited	55	January, 2020	
	Lakdhanavi Bangla	52.2					
	Desh Energy Chandpur	200		Payra LNG Power Plant	3600	1st phase-December, 2022 2nd phase-December, 2023	[11]
	Doreen Power Generations	165					
Gas Turbine	Meghnaghat	450	[15]				
	Ashuganj	146	[13]				
	Haripur	360					
	Golpara	265					
	Mymensingh	210					
	Siddhirganj	240					
Gas Engines	Baraka Power Ltd.	51	[16]				
	Dhaka	7					
	Gazipur	53					
	Gopalganj	100					
	Maona	35					
	Raozan	240					
	Ghorashal Regent	108					
	Baghabari	50					
Hydroelectric	Karnafuli	230	[17]				

Continued

	Teknaf	200
Solar PV	Sutiakhali	50
	Mymensingh	32
Nuclear	Rooppur Nuclear Power Plant	2400

Table 3. Electricity production & installed capacity [2].

							Average annual growth rate (%)
	1980	1990	2001	2008	2012	2014	2001 to 2014
Capacity of electrical plants (GWe)							
Thermal	0.91	2.29	3.48	4.972	7.88	9.60	8.12
Hydro	0.08	0.23	0.23	0.23	0.22	0.22	−0.34
Nuclear	0	0	0	0	0	0	
Wind					0	0	
Geothermal	0	0	0	0	0	0	
Other Renewable					0	0	
Total	0.99	2.35	3.711	5.202	8.100	9.82	7.78
Electricity Production (TWh)							
Thermal	2.07	7.17	14.48	23/361	34.341	41.607	8.46
Hydro	0.58	0.88	1.08	0.949	0.776	0.588	−4.57
Nuclear	0	0	0	0	0	0	
Wind					0	0	
Geothermal	0	0	0	0	0	0	
Other Renewable					0	0	
Total	2.65	7.73	15.56	24.31	35.118	42.195	7.98
Total Electricity consumption (TWh)		4.704	14.002	22.622	30.098	40.296	8.47

2.4. Energy Statistics

Current electricity production and installation capacity of Bangladesh are described here by **Table 3**, where electricity transmission losses are not deducted.

2.5. Electricity Access across the Population

Bangladesh has made significant progress in access to electricity as its electrification coverage reached 88% in 2017. The World Bank mentioned that among the countries with the largest population without access to electricity Bangladesh, Kenya, Myanmar, and Sudan have made the most progress. World Bank, Sustainable Energy for all database shows the progress in the following **Figure 3** [18].

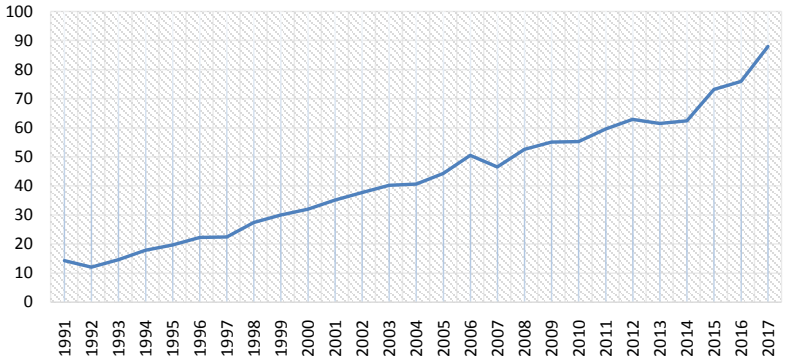

Figure 3. Electricity access across the population (%) corresponding to year.

2.6. Energy Conversion

Energy conservation is one of the most important issues of the sector due to economic and environmental reasons. However, until a very recent past no serious attempts were made to take up and implement energy conservation programs which have been given due importance in the National Energy Policy of Bangladesh (1996) [7].

2.7. Specifications System Loss

System loss of more than 4% in power generation is not acceptable. It has been stated that the average system loss of power generation by the PDB is 6.35%. The government will plan to reduce system loss to a specified limit [7].

2.8. Generation Lag

In the past situation, Bangladesh faced an enormous electricity shortage that affected non-agricultural employment. So, there was a great energy gap between peak demand and maximum energy generation. Those gaps are said to be the generation lag. In Bangladesh, the present government promised to ensure the continued supply of electricity to all the citizens by the year 2021. According to the Power System Master Plan (PSMP) 2010, the forecasted demand for the power based on 7% GDP growth rate shows the only Nuclear Power Plant can full fill the demand of the nation, that is illustrated in **Figure 4** by showing the exponential increase of peak demand (MW) [19].

2.9. Energy Import

In order to fill up the gap in between demand and generation, every year Bangladesh imports power from neighbor country. Which costs huge. The import of electricity from India and Bhutan are worth exploring. Myanmar has satisfactory gas reserves. Bangladesh could negotiate for import of gas from Myanmar [7].

3. Government Vision

3.1. Brief Story

Bangladesh is a country with no shortage of well-written policies. It is the

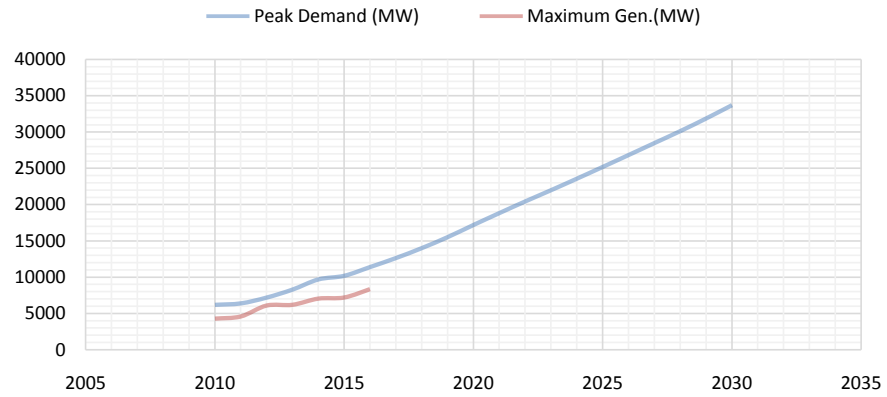

Figure 4. Difference in between peak demand & maximum generation.

implementation of these where the problem begins. This is not only an isolated problem for Bangladesh alone. Sometimes the reality shows that that convincing an idea is often easier than putting it into practice. The energy sector have is no different in having some well-constructed ideas and policies. Some of the policies of recent years are given below [20]:

- National Energy Policy-2004,
- Renewable Energy Policy of Bangladesh-2008,
- The Sixth Five-year plan of Bangladesh (2011-15)-2011,
- Perspective plan of Bangladesh (2010-2021) Vision 2021-2012,
- The National Sustainable Development Strategy-2013,
- Intended National Determined Contributions-2015,
- The Seventh Five Year Plan (2016-2020)-2015,
- Energy Efficiency and Conservation Master Plan up to 2030-2015,
- Power System Master Plan-2016.

3.2. The Power Sector Master Plan (PSMP)-2016 (Vision 2041)

The PSMP is a document that aimed to assist the Bangladesh Government in formulating an extensive energy and power development plan up to the year 2041. It highlights the country's desire to become a high-income country by 2041, so the quantity and quality of the power infrastructure must also reflect that status. Due to the upcoming depletion of domestic gas the Plan highlights the issues of sustainable development harmonizing with economic optimization, improvement of power quality for the developing high-tech industries and the operation and maintenance of power plants to be all addressed holistically. It should be noted that the current form of the paper is not set in stone and further development is likely to take place. The factor of energy subsidies was also highlighted as being a tough challenge due to the concern that a drastic increase of fuel and energy prices may trigger another negative effect on the national economy. A meticulous analysis is required to find the best route to attaining the balance of energy sustainability and economic growth. The 2016 version of the PSMP covers why that the energy development predicted in the 2010 PSMP is

not on track. It cited various assumptions about expected sources of base load energy having changed, and the vast increase of oil based rental power plants, and the lack of control over their power production. This has created a very unstable production network with no real central control to dictate country wide production schedules. The plan lays out five key goals of the vision 2041 [20]:

- Enhancement of imported energy infrastructure and its flexible operation.
- Efficient Development and utilization of domestic natural resources (gas and coal).
- Construction of a robust, high-quality power network.
- Maximization of green energy and promotion of its introduction.
- Improvement of human resources and mechanisms related to the stable supply of energy.

3.3. Energy Mix Concept

Due to the low current state of primary energy resources, demand is not being met. In this context, the Government is formulating the "Five-Fuel strategy," of which the priorities are given below [2].

- Undertake immediate exploration of hydrocarbon and identify additional reserves that can meet the growing demand of gas by all consumer sectors.
- Develop alternative commercial energy supplies suitable for power generation, especially coal, to ease the burden of fast-growing electricity demand on gas resources. Thus, a two-fuel (gas and coal) strategy is required for both resource diversification and energy security.
- Ensure efficient use of energy by using energy–saving appliances, plants and equipment in order to effectively increase the stock of available energy supplies.
- The resource potential of renewable energy is significantly larger than its present consumption and is a promising source of clean, convenient energy supply, especially in rural areas.
- Considering the limitation of fossil fuel supplies, nuclear fuel could be a potential energy option for the country, as it is a proven technology for economic, reliable and sustainable electricity generation.

At present, almost 88% of the country's power is dependent on gas and almost 50% of the consumed commercial energy is used for power generation. To ensure energy security more balance is needed. Present energy mix in Bangladesh and target mix of energy is shown here by **Table 4** and also those data are compared with the global position [7]. Projection of the primary energy supply shown by the **Table 5**.

3.4. Electricity Supply Expansion Plan

In order to decrease the pressure on natural gas, oil and biofuel it is wiser to develop alternative plan so that ensure the efficient use of different energy sources. That's why their Power System Master Plan-2016 suggests a projection of energy supply.

Table 4. Energy mix comparison in between Bangladesh and global [7].

Energy	Bangladesh		Global	
	Current (%)	2021 (%)	Current	2030
Gas	87.5%	30%	18%	28%
Oil	6%	3%	10%	5%
Coal	3.7%	53%	37%	38%
Hydro	2.7%	1%	17%	4%
Nuclear	0%	10%	17%	19%
Renewable	0.5%	3%	1%	6%

Table 5. Projection of primary energy supply [4].

Primary Energy Sources	2014		2041		Annual growth rate (2014-2041)
	kote	(Share%)	kote	(Share%)	
Natural Gas	20,726	56	50,149	38	3.3%
Oil	6263	17	32,153	25	6.2%
Coal	1361	4	26,273	20	12.7%
Nuclear Power	-	-	11,942	9	-
Hydro, Solar, Wind Power and Others	36	0	197	0	6.5%
Biofuel and waste	8449	23	4086	3	−2.7%
Power (Import)	377	1	6027	5	10.8%
Total	36,888	100	130,827	100	4.8%

4. Rooppur Nuclear Power Plants

4.1. History

Bangladesh is in the stage to become the 33rd Nuclear Power producing nation. The Rooppur Nuclear Power Plant (RNPP) is expected to generate 2400 MW of power, helping the nation to address the expanding demand for electricity. The project is done by the financial and technical support of the Russian State Energy Commission (ROSATOM). The idea of building a nuclear power plant was developed in the year 1961. Only after the chosen primary site, Pakistan government shifted the nuclear power plant project to Karachi. After independence, the government of Bangladesh again took over the project and decided to set up a nuclear power plant that has a capacity of 200 MW.

Some of the key milestones of Bangladesh national Power program is given below here [2]:

- 1963: Rooppur site selected for implementation of Nuclear Power Plant (NPP).
- 1971-78, 1987-88: Feasibility studies for site and first NPP conducted. Further feasibility studies for site and first NPP conducted.
- 1996: National Energy Policy identifies nuclear power as an option.
- 2000: BANPAP approved by the government.

- 2010: National Parliament approves first NPP project and new structure for NP program development (equivalent NEPIO) were formed (National Committees, Technical Committee, Working Group).
- 2011: IGA with Russian federation signed for the first NPP with two VVER units, each of 1000 MW.
- 2012: Bangladesh Atomic Energy Regulatory Act 2012 was passed in the National Parliament on 19th June 2012.
- 2013: Bangladesh Atomic Energy Regulatory Authority was formed as a separate entity on 12th February 2013.
- 2015: General contract was signed with Russian Federation for main stage construction of Rooppur NPP.
- 2016: Inter-Government State Credit Agreement for financing the main stage construction of Rooppur NPP.

4.2. Why Nuclear Power?

4.2.1. Heating Value

Bangladesh needs a stable and powerful alternative energy source to produce electricity. Alternative energy source means the type of source which is alternative to fossil fuel. Among all Nuclear Energy is the most effective and powerful. At this energy source is capable of producing enormous power ensuring the least fuel consumption. A comparison between heating values of different fuels are given below in **Table 6** [5].

4.2.2. CO_2 Emission

Greenhouse gases (Carbon dioxide, nitrous oxide, methane) surround the Earth like a blanket. As we use to burn more coal, natural gas, and oil, the blanket becomes excessively thick, dense, and less likely to allow heat to escape. Heat gets trapped inside the blanket of greenhouse gases and the Earth becomes too warm. Nuclear power is a much better choice than conventional gas or coal-based power plant. Where Nuclear power plants emit greenhouse gases less than any other, **Figure 5** gives a clear idea about this statement.

4.2.3. Comparison among Different Methods of Energy Generation

The nuclear power plant is relatively a good choice when we are only on CO_2

Table 6. Heating value of different fuels.

Fuel	Heating Value (MJ/kg)
Fire Wood	16
Brown Wood	9
Black Coal (Lower grade)	13 - 20
Black Coal (Higher grade)	24 - 35
Natural Gas	40
Crude Oil	45
Uranium	500,000

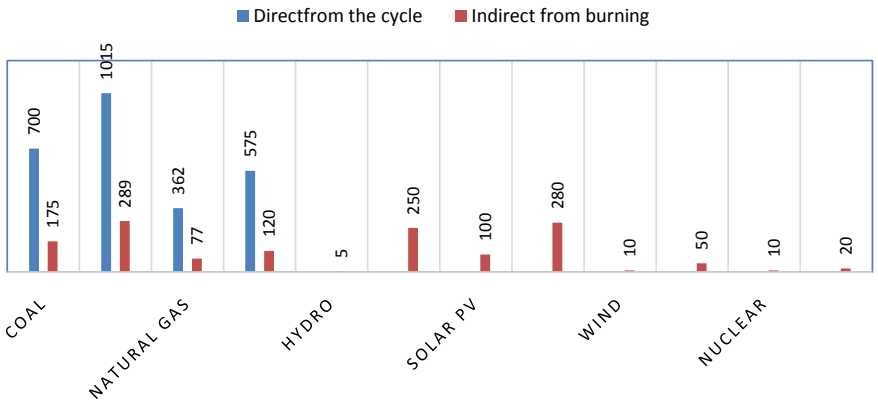

Figure 5. Greenhouse gas emission from different energy sources [5].

emission and heating value produced by burning the nuclear fuel. But Nuclear power plants are relatively expensive to build. Especially it takes 75% cost only for machinery, setup and capital cost. So the nuclear power plant is cheaper to run. **Table 7** shows a comparison among different methods of energy generation technologies.

4.3. Nuclear Power Development Strategy

4.3.1. Target Power Production

Bangladesh is evolving an energy mix diversification, where nuclear is one of the best choices. Right now the Bangladesh government has the plan to set up 2 units of Rooppur Nuclear Power Plan, described by the **Table 8.**

4.3.2. Project Funding

On 2 November 2011, the Government of the Russian Federation and the Government of the People's Republic of Bangladesh signed an agreement on cooperation for the construction of an NPP on the territory of the People's Republic of Bangladesh. An agreement was signed on 15 January 2013 between the Government of the People's Republic of Bangladesh and the Government of the Russian Federation on the extension of a state export credit to the Government of Bangladesh for financing of the preparatory stage for construction of an NPP in the People's Republic of Bangladesh. The credit shall be used by Bangladesh during 2013-2016 [2].

4.3.3. Project Management

Bangladesh Atomic Energy Commission (BAEC) has been appointed as the owner organization of NPP by:

- The prudential order 15, 1973,
- Bangladesh Nuclear Power Action Plan, 2000,
- Inter-Government Agreement (IGA) between Russian Federation and Bangladesh, 2011,
- Nuclear Power Plant Act, 2015 and
- All other Relevant policy documents.

Table 7. Comparison among different methods of energy technique [5].

Technology	Time (Unit)	Time (lead)	Cost (Capital)	Cost (Operational)	Fuel Necessity	Sustainability
CCGT	Medium	Short	Low	Low	High	NO
Nuclear	Huge	Long	High	Low	Low	OK
Coal	Large	Long	High	Low	Medium	NO
Hydro	Huge	Long	Very High	Very Low	N/A	OK
Wind	Small	Short	High	Medium	N/A	OK

Table 8. Planned nuclear power plants [2].

Power Station	Type	Capacity (MW)	Expected Construction Year	Expected Commercial Year
Unit-I	VVER	1200	2017	2023
Unit-II	VVER	1200	2018	2024

Nuclear Power Company of Bangladesh Limited (NPCBL) is the operating organization which clearly reflects in NPP Act 2015 [2].

4.4. VVER-1200 (Generation III+ Design) & Safety

4.4.1. VVER

The VVER is a pressurized water reactor (PWR), the commonest type of nuclear reactor worldwide, employing light water as coolant and moderator. However, there are some significant differences between the VVER and other PWR types, both in terms of design and materials used. Distinguishing features of the VVER include the following [21]:

- Use of horizontal steam generators,
- Use of hexagonal fuel assemblies,
- Avoidance of bottom penetrations in the VVER,
- Vessel,
- Use of high-capacity pressurizers.

4.4.2. VVER Generations

VVER is one of the oldest type reactor technology used in nuclear technology by the Russian. Starting from 1964 (Gen I), VVER now is in nuclear market with its new technology which is called generation III+ VVER-1200 with lots of improvement. Different generations of VVER reactor are mentioned here by **Table 9**.

4.4.3. VVER-1200

Main principles of VVER-1200 (AES-2006) design are [21]:

- Maximum use of proven technologies,
- Minimum cost and construction times,
- Balanced combination of active and passive safety system in general to manage beyond basis accidents,
- Reduction in the influence of human factors on overall safety.

Table 9. VVER generations [21].

Gen I (1964-1966) VVER	Gen II (1966-1980) VVER-440	Gen II/Gen III (1980-2006) VVER-1000	Gen III+ (2006-) VVER-1200
V-210 Russia, Novovoronezh1	V-179 Russia, Novovoronezh 3-4	V-187 Russia: Novovoronezh 5	V-392M Russia, Novovoronezh II 1-2
V-365 Russia, Novovoronezh1	V-230 Russia, Kola 1-2 East Germany, Greifswald 1-4 Bulgaria, Kozloduy 1-4 Slovakia, BohuniceI 1-2	V-302 Ukraine, South Ukraine 1	V-491 Russia, Baltic 1-2 Leningrad II 1-2 Belarus, Belarus 1
	V-213 Russia, Kola 3-4 Ukraine, Rovno 1-2 Hungary, Paks 1-4 Czech Rep., Dukovany 1-4 Finland, Loviisa 1-2 Slovakia, Bohunice II 1-2 Mochovce 1-2 Mochovce 3-4	V-338 Ukraine, South Ukraine 2 Russia, Kalinin 1-2	
	V-270 Armenia, Armenia-1 Armenia-2	V-320 Russia, Balakovo 1-4, Kalinin 3-4, Rostov 1-2, Rostov 3-4 Ukraine, Rovno 3-4, Zaporozhe 1-6, Khmelnitski 1-2, South Ukraine 3 Bulgaria, Kozloduy 5-6 Czech Rep, Temelin 1-2 V-428 China, Tianwan 1-2, Tianwan 3-4 V-412 India: Kudankulam 1, Kudankulam 2 V-466 Iran: Bushehr 1	

4.4.4. Fundamental Safety Functions

1) Control of Reactivity

- Preventing uncontrolled reactor power increase.
- Ensuring fast safe shutdown of the reactor when needed [21].

2) Decay Heat Removal

- Cooling of the shutdown reactor.
- Cooling of used nuclear fuel [21].

3) Containment of Radioactive Material

- Preventing significant radioactive releases to the environment [21].

4.4.5. Protection from External Impacts

1) Seismic Loads

Protection against seismic hazards is provided taking into account the site-

specific seismic conditions. For instance, in the terminal 3 - 4 VVER-1200 offer, the buildings are designed to stay intact if the horizontal maximum ground acceleration caused by an earthquake does not exceed 0.25 g [21].

2) Hurricanes & Tornados

Safety-related components are designed to cope with a wind load corresponding to a wind velocity of 30 m/s at a height of 10 m. Design loads are those corresponding to a whirlwind of class 3.60 according to the Fujita scale [21].

3) Aircraft Crash

This VVER-1200 is designed to withstand a small airplane crash, with a design basics aircraft weight of 5.7 t. Protection against the impact of larger aircraft, depending on customer requirements, can be achieved by increasing the thickness of the outer containment wall and of some other buildings. A large (400 t) passenger plane crash was included in the design basis for the terminal 3 - 4 offer, and the ability to withstand such a crush demonstrated by detailed analysis supported by model testing [21].

4) Snow and Ice Loads

Design peak snow load is 4.1 kPa [21].

5) External Explosions

VVER-1200 safety-related components are designed taking into account a shock wave arising from an external explosion. The pressure at the shock wavefront is taken to be 30 kPa, with a compression stage time of 1 second [21].

4.5. Electric Grid Development

PGCB maintained the gridline of Bangladesh, where different power generation company contributes their power either in 230 kV or 132 kV line. At present 10,000 MW is the maximum load that can be handled by the grid line. According to the plan, a 400 kV line is going to be hooked up in order to import power from India. At present, the dependable generation capacity of the country will be about 12,000 MW against a maximum demand of about 11,000 MW in 2017. But the contribution of nuclear power will be about 2000 MW by the year 2020 and will be increased by about 5000 MW in 2030. So the installed capacity is projected to increase about 33,000 MW by 2030. So, PGCB needs to upgrade the national grid [2].

4.6. Public Concern

4.6.1. Fuel Cycle & Waste Management

Bangladesh believes that a healthy market exists at the front end of the fuel cycle. Currently, all reprocessing plants are state-owned and any guarantee from a supplier would have the implicit or explicit agreement with the corresponding government. Based upon the existing nature of the nuclear business worldwide, Bangladesh is considering a long-term contract and transparent suppliers' arrangements with supplier(s) through backing of the respective government in order to ensure the availability of fuel for the nuclear power reactor of the country. Examples would be fuel leasing and fuel take-back offers, commercial offers

to store and dispose of spent fuel, as well as commercial fuel banks. On the other hand, at present, there is no international market for spent fuel disposal services [2].

4.6.2. Earthquakes

The number of earthquakes (magnitude between 4 and 6) occurred in the last decade inside the country or near the borders. That has raised awareness among the general public and the government. But the good news is these earthquakes are located far away from the Rooppur site [2].

4.6.3. Security of the Nuclear Materials

Nuclear materials will be strictly supervised by the government of Bangladesh. However, remains a certain concern due to the increasing terrorist activities in the region. However, the government of Bangladesh has not made any clear statements on the issues of non-proliferation policy and measures from the part of the government [19].

4.6.4. Shortage of U Resources

The world has around 5.47 million tU of uranium resources, costing approximately US$130/kgU to produce. Among them, just 30% are in Australia, about 14% in Kazakhstan, followed by 16% in Russia and Canada, and in South Africa, China, Niger, Brazil all of them have 5% in Uranium resources [22]. By comparison, Bangladesh's share 0.25%.

4.6.5. Power Plant Cost

We already noticed that the fuel is at high prices in the world market. Although for Nuclear Power Plant fuel only takes 20% of the total power plant cost. On the other hand, Capital cost of land, machinery and set up will take 75% (with interest) of total cost and 5% cost is reserved for maintenance cost [5]. Which seems like to be a huge cost Bangladesh have to carry out only for nuclear power plant set up. It can be said a high investment risk.

4.6.6. Cost of Electricity

It shows that the purchase, operation, and maintenance of plants at the generation stage, will lead to increased spending on the generation and consequent higher cost of power supply. Ultimately, the price per unit of electricity needs enhancement. Strong Energy Regulatory Commission will have to address these issues.

4.6.7. Water Supply

The Rooppur NPP site was chosen even before the creation of Bangladesh. At that time the Padma (Ganga) river was selected for the water supply source of the power plant. But when in 1975 India completed the Farakka barrage, it affected Bangladesh's water supply, including the river level in the area of the Rooppur NPP. Water supply is a really serious technological challenge for the Rooppur NPP, that likely to be resolved via a protected water-catchment area in

the Padma River [23].

4.6.8. Cyber Threats

The digital security system of Bangladesh is not safe enough. On 1st February 2017 a seminar was organized named "Entering the world of Nuclear Energy" about the cyber-security where Dr. Petr Topychkanov stated 'Digital security must be guaranteed. Generally, there may be a tremendous hazard. In the event, there is no activity taken and it ought to be taken as right on time as possible' [5].

4.7. Research & Development

Under the assistance of the International Atomic Energy Agency (IAEA), BAEC has engaged in lots of activities to develop not only the manpower for future work but also develop the nuclear power concept all over Bangladesh since 1960. BAEC built the country's largest nuclear research center called "Atomic Energy Research Establishment". Where the 3 MW TRIGA Mark-II research reactor has been operating especially for radioisotope production and developing manpower training projects.

For developing the manpower for a very complex and modern RNPP project, Bangladesh Government has developed a contract with the Russian Government to develop almost 2100 personnel for both technical and non-technical training purpose. In the same way, every year twenty students from Bangladesh are coming to Nuclear Engineering of MEPhI University for higher studies.

4.8. Public Acceptance

It was 1963 when the Rooppur site was selected for the nuclear power plant project. After a long gap in 2016 Inter-Government agreement was done for main stage construction of RNPP. Although there was a huge gap of time to implement the ideas in the real working field, but the local people are so concern about the power situation in that time of the country. They also thought in quiet differently that, the power station may create a huge job opportunity for them and also the overall developing of that specific area of the country. So, it was so much easy task for the Government to spread the Nuclear technology to all over the country.

But in general, will be always a political conflict with the anti-nuclear agenda. That makes some concerns on the public's minds. So BAEC and the Russian contractors arranged lots of awareness programs for the public. BAEC arranged international seminar which was inaugurated by the Honourable Prime Minister Sheikh Hasina. They also arranged art competitions, booklet distribution, opinion sharing meeting, etc. [2]. All of those attempts make a great sense in public the mind.

5. Conclusion

In order to make the world green and safe for the future generation with lots of

energy resources, every country should have to pick up the lifeline of Sustainable Energy. But huge technological advancement makes nuclear energy so much better than any other choices with huge energy production limelight and less GHG emission. So, in the first stage, there should be some confusion going on to the mind of local people. But, when the Rooppur Power Plant will provide the energy in the national grid system, then they will definitely say nuclear power is the best choice among all. This is not only for providing power for the near future, but also securing lots of families by providing job opportunities and make socio-economic development. By seeing the nation's vision and recent technological advancements on the nuclear side makes it so much easier choice for the country like Bangladesh to choose VVER-1200 for reducing the energy gap and ensuring the electricity to all the citizens in near future.

Conflicts of Interest

The authors declare no conflicts of interest regarding the publication of this paper.

References

[1] Rahman, L. (2015) Digital Bangladesh: Dreams and Reality. The Daily Star. https://www.thedailystar.net/supplements/24th-anniversary-the-daily-star-part-1/digital-bangladesh-dreams-and-reality-73118

[2] IEAE (2016) Country Nuclear Power Profiles Bangladesh. https://cnpp.iaea.org/countryprofiles/Bangladesh/Bangladesh.htm

[3] (2015) World Energy Statistics Asia. https://www.worlddata.info/asia/bangladesh/energy-consumption

[4] Bangladesh Power System Master Plan 2016. http://powerdivision.portal.gov.bd/sites/default/files/files/powerdivision.portal.gov.bd/page/4f81bf4d_1180_4c53_b27c_8fa0eb11e2c1/(E)_FR_PSMP2016_Summary_revised

[5] Sabhasachi, S., Koushik, R., Souvik, R., Asfakur, R.Md. and Zahid, H.Md. (2018) Rooppur Nuclear Power Plant: Current Status & Feasibility. *Journal of Mechanical Engineering*, **68**, 167-182. https://content.sciendo.com/configurable/contentpage/journals$002fscjme$002f68$002f3$002farticle-p167.xml https://doi.org/10.2478/scjme-2018-0033

[6] Taheruzzaman, M. and Janik, P. (2016) Electric Energy Access in Bangladesh. *Transactions on Environment and Electrical Engineering*, **1**. https://www.google.com/url?sa=t&rct=j&q=&esrc=s&source=web&cd=2&cad=rja&uact=8&ved=2ahUKEwiH_77br4jmAhUolIsKHcT9B_0QFjABegQIBRAB&url=https%3A%2F%2Fwww.researchgate.net%2Fpublication%2F306047475_Electric_Energy_Access_in_Bangladesh&usg=AOvVaw2jg8mCGseQqUQwWvTeewdN https://doi.org/10.22149/teee.v1i2.13

[7] General Economics Division Planning Commission, Government of the People's Republic of Bangladesh (2012) Perspective Plan of Bangladesh 2010-2021.

[8] Barapukuria Coal Power Plant, Global Energy Observatory (2014). http://globalenergyobservatory.org/geoid/40466

[9] CPGCBL (2018). http://www.cpgcbl.gov.bd

[10] NWPGCL (2019) Ongoing Projects. http://www.nwpgcl.org.bd

[11] NWPGCL (2018). http://www.nwpgcl.org.bd

[12] Power Plants around the World (2014) Oil- and Gas-Fired Plants in Bangladesh.

[13] Global Energy Observatory (2014) Ashuganj Gas Power Plant. http://www.apscl.gov.bd

[14] Global Energy Observatory (2014) Ghorasal Gas Power Plant.

[15] Power Plants around the World (2013) CCGT Power Plants in Bangladesh.

[16] Power Plants around the World (2014) Diesel and Gas-Engine Power Plants in Bangladesh.

[17] Global Energy Observatory (2014) Karnafuli Hydroelectric Power Plant.

[18] World Bank, Sustainable Energy for All (SE4ALL) Database from the SE4ALL Global Tracking Framework Led Jointly by the World Bank, International Energy Agency, and the Energy Sector Management Assistance Program. https://data.worldbank.org/indicator/EG.ELC.ACCS.ZS

[19] Karim, R., Karim, M.E., Muhammad-Sukki, F., Abu-Bakar, S.H., Bani, N.A., Munir, A.B., Kabir, A.I., Ardila-Rey, J.A. and Mas'ud, A.A. (2018) Nuclear Energy Development in Bangladesh: A Study of Opportunities and Challenges. *Energies*, **11**, Article No. 1672. https://www.scopus.com/inward/record.uri?partnerID=HzOxMe3b&scp=85051239091&origin=inward https://doi.org/10.3390/en11071672

[20] Power Division, Ministry of Power, Energy and Mineral Resources, Government of the People's Republic of Bangladesh (2016) Power System Master Plan 2016 Summary.

[21] The VVER Today: Evolution, Design, Safety, ROSATOM.

[22] OECD-NEA & IAEA, Uranium (2018) Resources, Production and Demand ("Red Book"). World Nuclear Association, the Nuclear Fuel Report 2015, 2017 & 2019.

[23] Topychkanov, P. (2017) Why the Bangladeshi Public Has Concerns over the Rooppur Nuclear Project. https://carnegie.ru/2017/02/27/why-bangladeshi-public-has-concerns-over-rooppur-nuclear-project-pub-68116

Call for Papers

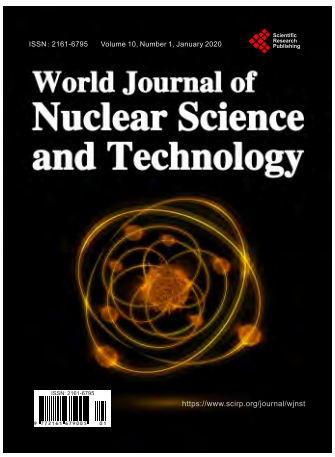

World Journal of Nuclear Science and Technology (WJNST)

ISSN 2161-6795 (Print) ISSN 2161-6809 (Online)
https://www.scirp.org/journal/wjnst

World Journal of Nuclear Science and Technology **(WJNST)** is an international peer-reviewed, open access journal publishing in English original research studies, reviews in all aspects of nuclear science and technology and its applications. Symposia or workshop papers may be published as supplements.

Editor-in-Chief

Prof. Andrzej Grzegorz Chmielewski

Editorial Board

Dr. Abdullah Aydin
Prof. Jiejin Cai
Prof. Ahmet Cengiz
Prof. Abdelmajid Choukri
Prof. Snezana Dragovic
Prof. Hardy Christian Ekberg
Prof. Juan-Luis François
Prof. Shilun Guo
Prof. Shaban Ramadan Mohamed Harb
Prof. Xiaolin Hou
Prof. Ning Liu
Prof. Man Gyun Na
Prof. Dragoslav Nikezic
Dr. Rafael Rodríguez Pérez
Prof. K. Indira Priyadarsini
Prof. Massimo Rogante
Prof. Vitalii D. Rusov
Dr. Chhanda Samanta
Prof. Kune Y. Suh
Prof. Wenxi Tian
Dr. Heiko Timmers
Prof. Marco Túllio Menna Barreto de Vilhena
Dr. Jun Wang
Dr. Leopoldo A. Pando Zayas

Subject Coverage

This journal invites original research and review papers that address the following issues. Topics of interest include, but are not limited to:

- Fuel Cycle and Isotopes
- Global Nuclear Security Technology
- Nonreactor Nuclear Facilities
- Nuclear and Chemical Waste Management
- Nuclear and Particle Physics
- Nuclear Cardiology
- Nuclear Energy
- Nuclear Engineering and Design
- Nuclear Fusion
- Nuclear Instruments and Methods
- Nuclear Magnetic Resonance Spectroscopy
- Nuclear Materials
- Nuclear Medicine and Biology
- Nuclear Medicine and Molecular Imaging
- Nuclear Physics
- Nuclear Science and Techniques
- Nuclear Structural Engineering
- Nuclear Track Detection
- Nuclear Tracks and Radiation Measurements
- Radiation Applications and Instrumentation
- Radioanalytical and Nuclear Chemistry
- Reactor and Nuclear Systems
- Reactor Science and Technology

We are also interested in short papers (letters) that clearly address a specific problem, and short survey or position papers that sketch the results or problems on a specific topic. Authors of selected short papers would be invited to write a regular paper on the same topic for future issues of the WJNST.

Notes for Intending Authors

Submitted papers should not have been previously published nor be currently under consideration for publication elsewhere. Paper submission will be handled electronically through the website. All papers are refereed through a peer review process. For more details about the submissions, please access the website.

Website and E-mail

https://www.scirp.org/journal/wjnst **E-mail: wjnst@scirp.org**

What is SCIRP?

Scientific Research Publishing (SCIRP) is one of the largest Open Access journal publishers. It is currently publishing more than 200 open access, online, peer-reviewed journals covering a wide range of academic disciplines. SCIRP serves the worldwide academic communities and contributes to the progress and application of science with its publication.

What is Open Access?

All original research papers published by SCIRP are made freely and permanently accessible online immediately upon publication. To be able to provide open access journals, SCIRP defrays operation costs from authors and subscription charges only for its printed version. Open access publishing allows an immediate, worldwide, barrier-free, open access to the full text of research papers, which is in the best interests of the scientific community.

- High visibility for maximum global exposure with open access publishing model
- Rigorous peer review of research papers
- Prompt faster publication with less cost
- Guaranteed targeted, multidisciplinary audience

Scientific Research Publishing

Website: https://www.scirp.org

Subscription: sub@scirp.org

Advertisement: service@scirp.org